Renewable and Sustainable Energy Reviews 211 (2025) 115328

Contents lists available at ScienceDirect

Renewable and Sustainable Energy Reviews

journal homepage: www.elsevier.com/locate/rser

Original research article

Efficient, affordable, carbon-neutral power: Advanced solid oxide fuel cell-electrolyzer system

Xinyi Wei [a,b,*,1], Shivom Sharma [a,1], Jan Van herle [b], François Maréchal [a]

[a] Industrial Process and Energy Systems Engineering-École Polytechnique Fédérale de Lausanne (EPFL), Rue de l'Industrie 17, Sion, CH-1950, Valais, Switzerland
[b] Group of Energy Materials-École Polytechnique Fédérale de Lausanne (EPFL), Rue de l'Industrie 17, Sion, CH-1950, Valais, Switzerland

ARTICLE INFO

Keywords:
Solid oxide fuel cell
CO_2 capture
Solid oxide electrolyzer
Oxy-combustion
Heat integration and valorization
Techno-economic optimization

ABSTRACT

The alarming increase in atmospheric carbon dioxide levels, primarily attributed to human-induced fossil fuel combustion for power generation, underscores the urgency for sustainable solutions. The solid oxide fuel cell (SOFC) is a promising candidate for clean power and heat production. This study introduces an innovative system integrating SOFC with solid oxide electrolyzer cells (SOEC) to enhance CO_2 capture. Traditionally, the SOFC system converts about 85% of the fuel into electricity, with any unconverted fuel undergoing combustion, yielding water and CO_2. In this study, an enhanced SOFC system equipped with various CO_2 capture technologies has been evaluated, including post-combustion capture through amine absorption and membrane separation and burner oxy-combustion with pressure swing adsorption for air-to-oxygen separation, combined with SOEC for oxygen production from water and CO_2. Criteria such as efficiency, costs, CO_2 capture rate, and purity have been used for evaluation. Notably, the innovative SOFC-SOEC configuration achieves 100% CO_2 capture rate and purity. While the efficiencies of different integrated SOFC systems are comparable, membrane separation exhibits lower CO_2 capture rates, pressure swing adsorption results in decreased purity, and amine absorption requires a more substantial investment. Interestingly, the active area required for the SOEC is a mere 1.3% of the SOFC active area. The novel SOFC-SOEC system has proven to be a compact, long-term, and cost-effective solution, showing significant potential in advancing the transition towards cleaner and more sustainable power generation.

1. Introduction

The United Nations Sustainable Development Goals (SDGs) have targeted reducing CO_2 emissions by the year 2050. Central to achieving these targets is the energy transition to alternative green energy sources, which not only supports SDG 7 (affordable and clean energy) but also aids in accomplishing SDG 13 (climate action), which calls for urgent actions to prevent climate change and its impacts [1,2]. In 2023, coal-fired power plants accounted for over one-third of the global electricity supply. Approximately 8536 million tonnes (Mt) of coal were consumed during the year, with the majority of this usage concentrated in the electricity generation sector [3–5]. Coal combustion has been widely acknowledged as a significant contributor to climate change and has shown negative impacts on human health [6]. Thus, it is essential to develop technological solutions with higher efficiency and lower CO_2 emissions to meet the future energy demand of industry and society [7,8].

In order to shift from the coal-based traditional power plants, several countries are focusing on the installation of photovoltaic (PV) panels and wind turbines [9,10]. Renewable energy production has intermittency and variability, which necessitates that excess renewable energy has to be stored for short- or long-term use (batteries and green fuel production). Despite the rapid deployment of renewable energy installations, addressing the energy needs of fast-growing economies remains a significant challenge. Additionally, the variability in the energy supply may require grid operators to increase re-dispatches, thereby compromising energy security and independence.

While renewable energy is essential for reducing CO_2 emissions, CO_2 capture technologies are pivotal, particularly when renewable sources are developing slowly or where fossil fuel infrastructure persists. CO_2 capture enables the continued use of existing energy infrastructures while reducing the environmental impacts. This approach serves as an energy transitional strategy, facilitating gradual shifts

* Corresponding author at: Industrial Process and Energy Systems Engineering-École Polytechnique Fédérale de Lausanne (EPFL), Rue de l'Industrie 17, Sion, CH-1950, Valais, Switzerland.
E-mail address: xinyi.wei@epfl.ch (X. Wei).
[1] Contributed equally to the paper.

https://doi.org/10.1016/j.rser.2025.115328
Received 8 November 2023; Received in revised form 24 December 2024; Accepted 2 January 2025
Available online 15 January 2025
1364-0321/© 2025 The Authors. Published by Elsevier Ltd. This is an open access article under the CC BY license (http://creativecommons.org/licenses/by/4.0/).

Abbreviations	
AOG	Anode off gas
BECCS	Bioenergy with carbon capture and storage
CAPEX	Capital cost
CC	Combined cycle
CCS	Carbon capture and storage
CHP	Combine heat and power
CP	Connection point
DC	Direct current
FU	Fuel utilization
HP	Heat pump
ICE	Internal combustion engines
KPI	Key performance indicator
LHV	Lower heating value
MEA	Monoethanolamine
MILP	Mixed integer linear programming
OPEX	Operating cost
PEM	Proton exchange membrane
PSA	Pressure swing adsorption
RC	Rankine cycle
rSOC	Reversible solid oxide cells
SDG	Sustainable Development Goals
SH	Super-heating
SOEC	Solid oxide electrolyzer
SOFC	Solid oxide fuel cell

Nomenclature	
Symbol	Description
AF	Annualization Factor
α	Scaling factor
$CAPEX_{\text{ref}}$	Reference capital cost
$CEPCI_{2024}$	Chemical Engineering Plant Cost Index for 2024
$CEPCI_{\text{ref}}$	Chemical Engineering Plant Cost Index for reference year
i	Interest rate
LHV_{fuel}	Lower heating value of the fuel
n	Equipment lifetime (years)
P_{BOP}	Power consumed by the balance of plants
P_{SOEC}	Power consumed by the SOEC stack
P_{SOFC}	Power output from the SOFC stack
$\dot{m}_{\text{fuel}}$	Mass flow rate of the fuel
S	Size of the process
S_{ref}	Reference process size
η	Electrical efficiency of the SOFC system

towards more sustainable energy systems without causing disruptions that could affect energy supply and economic stability. Therefore, a comprehensive literature review is crucial for understanding conventional power generation technologies and their challenges. Identifying research gaps and evaluating other power generation technologies that could be integrated with CO_2 capture mechanisms is imperative. The aim is to assess both the performance and economic viability of these systems. The insights gained from this study are vital for both academic research and industrial applications, ultimately contributing to long-term sustainability goals.

2. State of the art

This section reviews various power generation technologies, highlighting their advantages and disadvantages. Further, potential power generation technologies are explored, and different CO_2 capture technologies are examined to identify potential research gaps and the contributions of this study.

2.1. Conventional power production technologies

Internal combustion engines (ICE) are widely used as a conventional power generation technology utilizing both liquid and gaseous fuels. They are economically viable, durable, and can operate in combined heat and power (CHP) mode [11,12]. Residential-scale CHP systems employing ICE have been extensively researched [13,14]. The electrical efficiency of ICE (35%–45%, for large diesel and gas engines) is comparable to that of other similarly sized power plants [15], and the thermal efficiency is significantly influenced by weather conditions. Nevertheless, ICE presents significant challenges, including a high likelihood of catastrophic failures, poor fuel consumption, and emissions of pollutants such as nitrogen oxides (NO_x), soot particulates, and CO. Efforts are underway to develop green fuels for ICE, such as e-fuels and pyrolysis fuel [16], control strategies for emissions [17,18], and to improve combustion efficiency [19]. A comparative study has reported that an ICE using diesel has an exegetic efficiency of 22.36%, while a proton exchange membrane (PEM) fuel cell achieves an exergetic efficiency of 40.34% [20]. Therefore, despite advancements, ICE technology poses a significant challenge in achieving high electrical efficiency, and ongoing improvements may not be sufficient to overcome the inherent limitations, especially when compared to fuel cell technology.

Gas turbines have witnessed a surge in popularity recently, and this trend is expected to continue in the near future [21]. This popularity can be attributed to their relatively high power-to-weight ratio, multi-fuel compatibility, fast startup times, and reduced manpower requirements [22]. Industrial gas turbine systems typically target an efficiency of around 30%–35%, while mini- or micro-gas turbines often achieve efficiencies of less than 30%. To enhance their efficiencies, several modifications to the gas turbine cycle have been attempted, including increasing the turbine inlet temperature, incorporating waste heat recuperation through steam or water injection, and reducing air inlet temperature [23]. Further, the performance of gas turbines is significantly influenced by ambient conditions [24]. Additionally, the deployment of gas turbines in quieter neighbourhoods continues to be restricted by noise regulations [23].

The integration of a Brayton cycle (gas turbine) with a Rankine cycle (steam) is known as a combined cycle (CC). The utilization of waste heat from the Brayton cycle exhaust to power the Rankine cycle results in improved power generation with an overall efficiency exceeding 50%. The flexible operation, lower installation cost, quick installation, and high availability of CC power plants make it a promising technology [25]. With a total efficiency of 53.5% (with high-quality heat), CC power plants produce electricity at a lower cost compared to traditional steam power plants [26]. Performance enhancement strategies for CC power plants have been investigated in several studies, which include optimizing firing temperatures and enhancing partial load efficiency [27–31]. Nevertheless, exergy loss analysis in CC power plants indicates that the thermal combustion exergy losses are dominant, and decreasing these losses remains a challenging task.

Although internal combustion engines, gas turbines, and combined cycle power plants offer various advantages in efficiency and adaptability, they still present notable challenges, including high emissions,

dependency on fuel types, and sensitivity to environmental conditions. These limitations underscore the importance of exploring alternative power generation technologies that could potentially offer solutions without these drawbacks. The following section delves into emerging technologies that could enhance energy efficiency, offer operating flexibility, and reduce the environmental impact associated with traditional technologies, showing a promising market for future energy strategies.

2.2. Emerging technologies in power generation

Biomass is recognized as a promising renewable energy source with the potential for negative emissions, particularly when combined with carbon capture technologies. Zhao et al. [32] investigate its viability as a sustainable feedstock for refinery decarbonization. The study emphasizes that biomass can effectively sequestrate CO_2 during its growth phase, serving as a carbon-reducing input when transformed into bioenergy and chemical feedstocks. Such capabilities are particularly critical in facilitating the transition to lower-carbon alternatives in the transportation sector that is challenging to electrify.

Fajardy et al. [33] assess the economic viability of bioenergy with carbon capture and storage (BECCS) within climate stabilization frameworks. Their findings suggest that BECCS significantly lowers the costs of achieving global warming targets, primarily as it serves as a backstop technology, becoming economically feasible when CO_2 prices reach approximately 240 $/ton. Nonetheless, the large-scale implementation of BECCS could be limited due to environmental and political challenges, despite its minimal impact on global agricultural commodity prices. Similarly, Silveira et al. [34] investigate the potential and obstacles to implementing BECCS in Brazil, where a well-established biofuel industry provides a theoretical basis for extensive BECCS deployment. The study reveals minimal technical barriers; however, it questions the economic viability of BECCS plants without secondary benefits, such as selling biofuel as a product. Additionally, the study highlights that significant challenges in CO_2 transportation could escalate costs, particularly if the technology is expanded beyond specific geographic locations.

While bioenergy holds promise, its practical deployment faces several challenges, including resource availability, land use, and economic viability. Effective integration of bioenergy into the energy systems also remains a concern. Therefore, it is crucial to investigate transitional solutions that offer high system efficiency without being constrained by resource or spatial limitations and demonstrate strong economic market potential. Solid oxide fuel cell (SOFC) technology has garnered significant attention due to its potential to reduce dependency on the electricity grid [35–39]. SOFC systems can generate electricity using either liquid or gaseous fuels. The modularity of SOFC systems and the integration with external fuel storage make them highly compatible and easily adjustable for different industrial power plant scales. Furthermore, SOFC operates at high temperatures (around 800 °C) and co-generates high-quality heat or steam, which can partially be utilized as a heat source within the system. Currently, the electrical efficiency of a state-of-the-art SOFC system is more than 60% [40], while the efficiency for combined heat and power (CHP) configurations can exceed 90%, positioning it as a highly promising power production technology. Since the maximum fuel utilization (FU) for SOFC is around 0.85, a burner is required to combust unconverted fuels downstream of the stack. While the burner provides additional heat from the SOFC system, it also results in more CO_2 emissions.

2.3. SOFC system power production with CO_2 capture

Solid oxide fuel cell (SOFC) is a promising technology for efficient power generation. To achieve net-zero greenhouse gas emissions by the year 2050, it is crucial to prioritize the integration of carbon capture and storage (CCS) technology [41] into the SOFC system. The captured CO_2 can securely be stored underground, making these operations nearly carbon-neutral or utilized in the methanation process to convert renewable electricity into green methane. Integrating CCS with power production, mainly when using biofuels, can render the process carbon-negative. This section reviews the literature on integrating various CO_2 capture technologies with SOFC systems to enhance their environmental sustainability. Technologies such as monoethanolamine (MEA) scrubbing, membrane systems, and pressure swing adsorption (PSA) will be discussed.

Traditional carbon capture technologies such as MEA have been utilized for decades due to their commercial availability and extensive operational experience [42]. The MEA process is predominantly used for CO_2 capture from post-combustion flue gases [43]. It offers several advantages, including strong reactivity, low solvent cost, and high weight-based absorption capacity [44]. Some studies are currently focusing on developing absorbents that combine the quick absorption rate and high loading capacity of MEA with low regeneration heat [45]. However, the use of MEA also presents significant drawbacks, such as considerable solvent loss due to its high volatility, limited saturation loading capacity, and high energy requirements for regeneration [46, 47]. Currently, industrial CO_2 absorption using aqueous MEA is typically conducted in large columns, unsuitable for industries requiring compact absorption units [48]. Furthermore, integrating them with coal-fired power stations has hampered the power output (around 20%) and diminished overall thermal efficiency [49].

Membrane-based gas separation has garnered attention as a promising technology for CO_2 separation from flue gases. This method offers several advantages, including reduced capital and operating costs [50], a compact system design, environmental friendliness, process flexibility, and integration with other separation technologies. Membrane types such as carbon [51], polycarbonate [52], polysulfone [53], and polyimide [54] offer excellent functionality and adaptability in structural configurations. The electricity price increases by 35% for 90% CO_2 capture from flue gases using advanced membranes [55]. Furthermore, increasing the pressure difference between the membrane's feed and permeate sides enhances separation efficiency and selectivity [56, 57]. However, challenges such as membrane fragility, manufacturing complexity, and high costs restrict their practical application [58,59].

Besides directly capturing CO_2 downstream of the burner, introducing oxygen directly into the burner to facilitate oxy-combustion can produce CO_2 and water. After condensation, CO_2 is automatically separated from water. Cryogenic distillation, a common industrial method for air separation and O_2 production, is energy-intensive and unsuitable for small-scale applications. However, O_2 can be produced through alternative technologies such as pressure swing adsorption (PSA) and solid oxide electrolyzers, which have gained significant standing in the oxygen production market, particularly for small-scale and low concentration applications [60].

PSA is typically designed for small- to medium-scale production capacities and is capable of producing 94% pure O_2 [60]. Oxygen production via PSA, which involves using an electrically powered air compressor and bed of adsorbent material, is well-documented in the literature. The PSA-based oxygen production's energy requirements are highly sensitive to process parameters, including adsorption pressure, adsorbent type, desorption pressure, and cycle time. However, a major challenge of employing PSA for O_2 production — that may be utilized in the burner — is the presence of N_2. It means that after oxy-combustion, a separation unit is still necessary to isolate CO_2 from N_2, depending on the purity requirements of the CO_2 product, which can increase the cost dramatically [61].

Electrolyzers are another technology for producing hydrogen, with oxygen as a co-product [62]. Currently, a total of 5 GW of electrolyzer capacity is deployed worldwide, showing its promising marketplace [63,64]. Alkaline electrolyzer (AEL), proton exchange membrane (PEM), anion exchange membrane (AEM), and solid oxide electrolyzer (SOEC) are the primary electrolyzer technologies available in the market. The alkaline electrolyzer is regarded as the most advanced industrial electrolysis technology. Its primary benefit is the affordable price

of the metal electrode. However, its efficiency in hydrogen production is relatively low. PEM electrolyzers offer several advantages, including high hydrogen purity, high current density, and compact size, but their production is hampered by the scarcity of critical raw materials. AEM combines the advantages of PEM and alkaline technologies without the use of expensive materials, though this technology still has a relatively low technology readiness level (TRL).

The SOEC (or reversible SOFC) has garnered significant interest for hydrogen production and is currently being developed and tested at several hundred kW scales. SOECs operate at high temperatures, typically between 500 and 850 °C, and exhibit high conversion efficiency [39,65]. Additionally, SOECs are capable of co-electrolysing CO_2 and steam [66]. Moreover, the oxygen produced from the electrolyzer can easily be adjusted in different quantities by varying the electricity input, CO_2, and steam amounts. Thus, it can be considered as an attractive option for supplying O_2 to the SOFC system burner.

2.4. Research gaps and study's contributions

SOFC systems are recognized for their high system electrical efficiency in power generation and flexibility in fuel types, including bio-based and conventional fuels. They offer a promising transient solution for enhancing energy security. However, SOFC has high conversion efficiency, it can only convert about 85% of fuel, and the remaining fuel is combusted in a burner. Thus, integrating CO_2 capture technologies is crucial to align with environmentally friendly practices. While numerous CO_2 capture technologies have been studied, further research is essential to identify effective integrations of these technologies with SOFC systems, each tailored to specific conditions and applications. Additionally, analysing both conventional and emerging CO_2 capture technologies is essential to identify potential market opportunities. SOFC systems operate at high temperatures, not only facilitating the heat requirements of CO_2 capture technologies if needed but also allowing for the reuse of waste heat in industries needing high temperatures or in the conversion of heat back into electricity. While comprehensive system modelling and integration studies, which focus on overall efficiency, are imperative, understanding the economic aspects of these technologies is also critical to assessing market competitiveness and identifying cost-driving factors, particularly for emerging technologies where future cost impacts remain uncertain.

In this study, various CO_2 capture technologies integrated with SOFC systems are examined. The methods are categorized into two types: first, traditional SOFC systems employing air in the burner for post-combustion, requiring CO_2 capture from exhaust gases, with MEA and membrane technologies considered. The second type involves SOFC systems utilizing pure O_2 for oxy-combustion, enabling automatic CO_2 separation without additional components. The oxygen sources include PSA, which extracts O_2 from the air, and an innovative method proposed in this study—utilizing a SOEC to generate oxygen. Notably, SOEC and SOFC can operate as the same stack under different conditions, forming a highly compact and modular power generation system with integrated CO_2 capture capabilities, eliminating the need for extra equipment. This approach facilitates scaling and simplifies facility setup, offering significant advantages. This study aims to explore the SOFC-SOEC system through comparative analysis with traditional CO_2 capture technologies, representing a novel approach to sustainable power generation. Given the novelty of the proposed system, extensive room for operational improvements exists. Therefore, multi-objective optimization is conducted, considering industrial constraints to enhance system performance.

Subsequently, all proposed systems incorporating various CO_2 capture technologies undergo a system analysis to facilitate comparisons. This analysis considers key performance indicators (KPIs) such as system efficiency, CO_2 purity, and CO_2 recovery rate. Additionally, the inclusion of a Rankine cycle aims to further enhance the electrical efficiency of each system. This comprehensive evaluation allows for an understanding of the trade-offs involved by considering all KPIs. Furthermore, a techno-economic analysis is performed, taking into account various costs, including capital cost (CAPEX), operating cost (OPEX), CO_2 taxation, and electricity production prices, to assess the market potential of these technologies.

Overall, this study aims to propose a novel SOFC-SOEC configuration and explore its potential while also assessing the viability and comparative advantages of integrating various CO_2 capture technologies within SOFC systems. It seeks to provide insights into optimizing performance and economic outcomes, thereby contributing to the advancement of sustainable power generation technologies.

3. Materials and methods

This section presents an overview of the different system layouts included in the study, providing a broad perspective on each case. It details the main parameters and assumptions used in modelling each configuration. Additionally, the optimization framework is introduced, outlining the objective functions with their respective rationales, listing the various constraints, and identifying the decision variables. Finally, the assumptions and main cost estimations employed in the techno-economic analysis are discussed.

3.1. SOFC systems general description

Fig. 1 presents the conventional design of the SOFC system, structured into four main modules within the process flow diagram. The initial module, highlighted in green colour, comprises the SOFC system that converts chemical energy into electricity. Here, fuel and water are mixed and heated by an external heater to reach the required temperature for the external reformer. This step is necessary as the SOFC stack cannot support full internal reforming without the potential damage. After the external reforming, the flow is further heated and directed to the stack's anode side to generate electricity. On the cathode side, fresh air not only supplies the required oxygen but also regulates the temperature within the stack, maintaining the temperature gradient between the stack's inlet and outlet. The anode outlet flows into the second module, the burner system, shown in red colour, where any unconverted fuel is combusted. The resultant flue gas then moves to the third module, the condenser system, coloured in orange. This module condenses water, which may be reused in the SOFC system after undergoing further purification if needed. The final module, the heat recovery system, depicted in blue colour, harvests the high-quality waste heat produced by the system, potentially employing a Rankine cycle for further energy recovery.

As introduced in the previous section, the conventional design utilizes air in the burner and lacks CO_2 capture modules. In this study, the SOFC system without CO_2 capture is considered as the base case, as presented in Fig. 2(a). Subsequently, four alternative cases for clean power production using SOFC systems with different CO_2 capture methods are analysed. These include two cases with post-combustion CO_2 capture, illustrated in Fig. 2(b), and two cases with oxy-combustion using O_2, depicted in Fig. 2(c). The performance of the integrated SOFC system with CO_2 capture is compared based on electrical efficiency, annualized capital and operating costs, and CO_2 capture rate and purity. Detailed descriptions of different cases can be found in Table 1.

3.2. Details of SOFC system with CO_2 capture technologies

As shown in Table 1, all SOFC system cases share two common modules: the SOFC system module and the burner module. Figs. 3(a) and (b) illustrate the detailed layouts of these modules. The methods of developing SOFC system models are well-established in many research studies [67–70]. The SOFC stack model used in this study was developed based on our group's published research studies, with the modelling procedure outlined and validated in Wang et al. [71] and

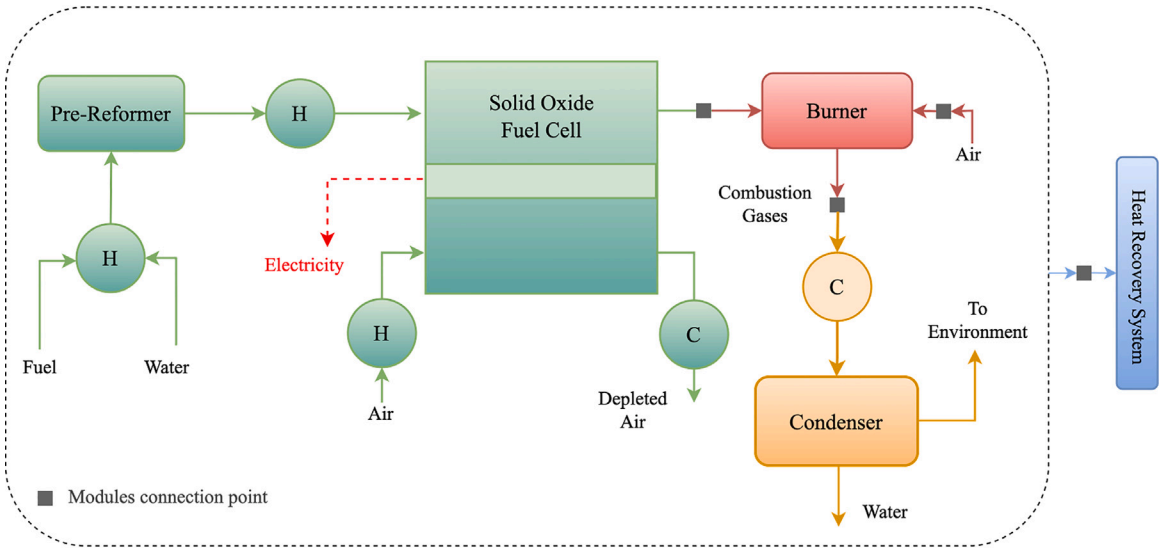

Fig. 1. SOFC system with burner, condenser and heat recovery system.

Table 1
Comparison of SOFC system cases and associated modules.

Case description	Configuration	Modules	
Base case	–		Burner, Condenser
Post-combustion CO_2 capture	Case 1A		Burner, MEA
	Case 1B	SOFC system	Burner, Membranes
Oxy-combustion and CO_2 separation	Case 2A		PSA, Burner, Condenser
	Case 2B		SOEC, Burner, Condenser

EU project [72]. As model validation is not the main focus of this study, and it has been done in our previous study [40,73], it is not detailed here. The main parameters used in the SOFC system models are summarized in Table 2. High single-pass fuel utilization is applied in SOFC stack operation, adhering to specifications provided by the stack manufacturer [74]. All models are developed in Aspen Plus v14.0.

3.2.1. Case 1: SOFC with post-combustion CO_2 capture

If post-combustion CO_2 capture is applied in the SOFC system, air is introduced into the burner, resulting in a product stream containing water, CO_2, and N_2. This stream is cooled to recover heat and condense water. Subsequently, the remaining CO_2 and N_2 mixture can be processed using the existing carbon capture technologies, such as MEA and membranes, to separate the CO_2.

For Case 1A (SOFC System + MEA), aqueous amine solutions, such as monoethanolamine (MEA) and activated methyl diethanolamine (aMDEA), are commonly used solvents for the chemical absorption of CO_2. To emphasize the modularity concept, individual system layouts for each module are presented instead of the full process flow diagram. Fig. 3(d) illustrates the schematic of CO_2 capture using MEA process. The complete system layout connects CP1 from Fig. 3(a) with CP2 from Fig. 3(b), and connects CP4 from Fig. 3(b) with CP6 from Fig. 3(d).

Firstly, the hot flue gases from the burner module are cooled, and water is condensed. The flue gases are then compressed and further cooled before entering the bottom of an absorption column, where an MEA solution is introduced at the top. Within the column, CO_2 reacts with the MEA, while the remaining gases are released into the environment. In the desorption column, CO_2 is separated from the MEA solution, which is then recycled back to the absorption column. Table 2 provides the design and operating parameters for the MEA process [75].

For the integration of membranes with the SOFC system (Case 1B), the full system layout is similar to Case 1A, with the only difference being the replacement of connection point CP6 with CP7. Fig. 3(e) illustrates a schematic of a two-stage membrane system for CO_2 separation from the flue gases. Initially, the flue gases are cooled to condense water. The compressed and cooled flow can enter any membrane stage, allowing flexibility in the separation process. Permeates from different stages can be combined to achieve the desired quality and flow rate of the product (e.g., CO_2), while retentates from various stages can be combined to meet the waste flow and quality requirements. Additionally, both retentate and permeate streams can (partially) be recycled to the same or different stages for enhanced separation. Fig. 3 depicts the optimized layout of the membrane system for separating flue gases generated from the air combustion of unconverted fuel in the SOFC. Table 2 provides the design and operating parameters for the two-stage membrane system [36,76,77].

3.2.2. Case 2: SOFC with oxy-combustion and CO_2 separation

There is potential to introduce oxygen directly into the burner to achieve oxy-combustion, enabling the direct separation of CO_2 downstream of the burner after water condensation, as shown in Fig. 2(c). Two options are available for supplying oxygen to the burner, including PSA and SOEC.

Connecting CP1 from Fig. 3(a) to CP2 from Fig. 3(b), CP4 from Fig. 3(b) to CP5 from Fig. 3(c), and CP8 from Fig. 3(f) to CP3 from Fig. 3(b) forms the configuration for Case 2A (SOFC System + PSA + Burner + Condenser). Fig. 3(f) illustrates a schematic of a two-bed PSA system. As PSA is a cyclic process, at least two beds are required for continuous O_2 production. Air is compressed before entering the adsorption bed, where N_2 is adsorbed onto the material, allowing high-purity O_2 to exit the bed. Once the material/bed becomes saturated with N_2, it undergoes a regeneration step. The conventional PSA cycle consists of four steps: pressurization, adsorption, blowdown, and purge. Table 2 provides the design and operating parameters for the PSA process [78].

The final option, Case 2B, is an innovative approach proposed in this study, where oxygen produced by the SOEC is supplied to the SOFC system burner. Similar to Case 2A, the connections among the SOFC

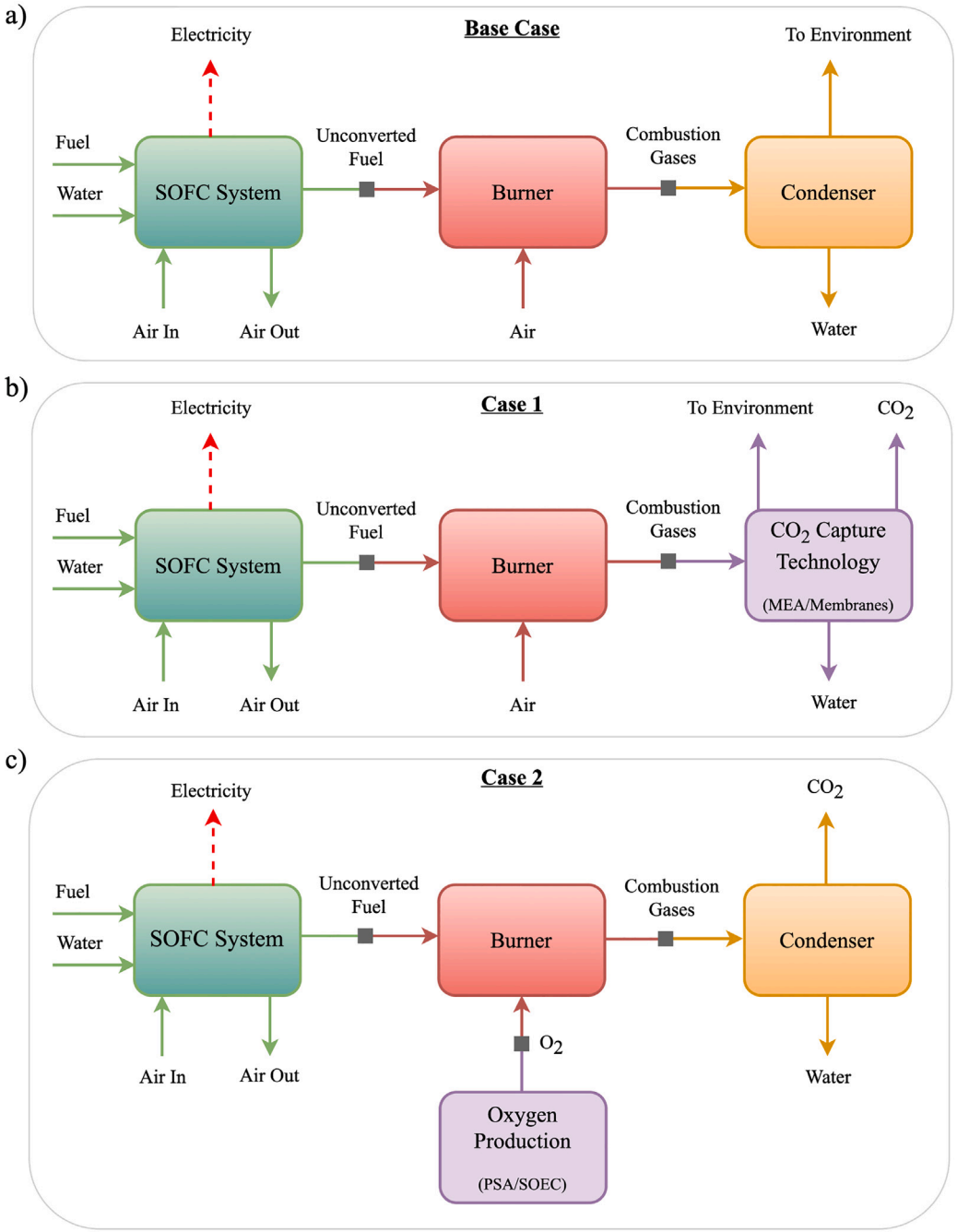

Fig. 2. (a) Base Case - Power production using SOFC, (b) Case 1 - Power production using SOFC with post-combustion CO_2 capture, and (c) Case 2 - Power production using SOFC with oxy-combustion and CO_2 separation.

system, burner, and condenser remain the same. However, the SOEC introduces four additional connections. A portion of the anode off-gas, primarily composed of CO_2 and steam, from the SOFC system is used as the input for the SOEC (CP1 from Fig. 3a linked with CP9 from Fig. 3g). Additionally, the cathode outlet from the SOEC, containing mainly H_2 and CO, is injected back into the SOFC system (CP10 from Fig. 3g linked with CP12 from Fig. 3a). Finally, the anode outlet (i.e., oxygen) from the SOEC is supplied to the burner (CP11 from Fig. 3g linked with CP3 from Fig. 3b). Table 2 presents details of design and operating parameters for SOEC system [79,80].

3.3. Multi-objective optimization

As this study introduces the novel concept of the integrated SOFC-SOEC system, it is interesting to focus on identifying optimal operating conditions to achieve optimal performance by considering multiple objective functions before comparing them with other system layouts, which are pretty conventional. To this end, multi-objective optimization has been conducted [40,67] using the OSMOSE tool [81,82]. OSMOSE employs a multi-objective genetic algorithm (MOGA) and performs heat cascade calculations. For optimizing the performance of the process model in flow sheeting software, OSMOSE is integrated with

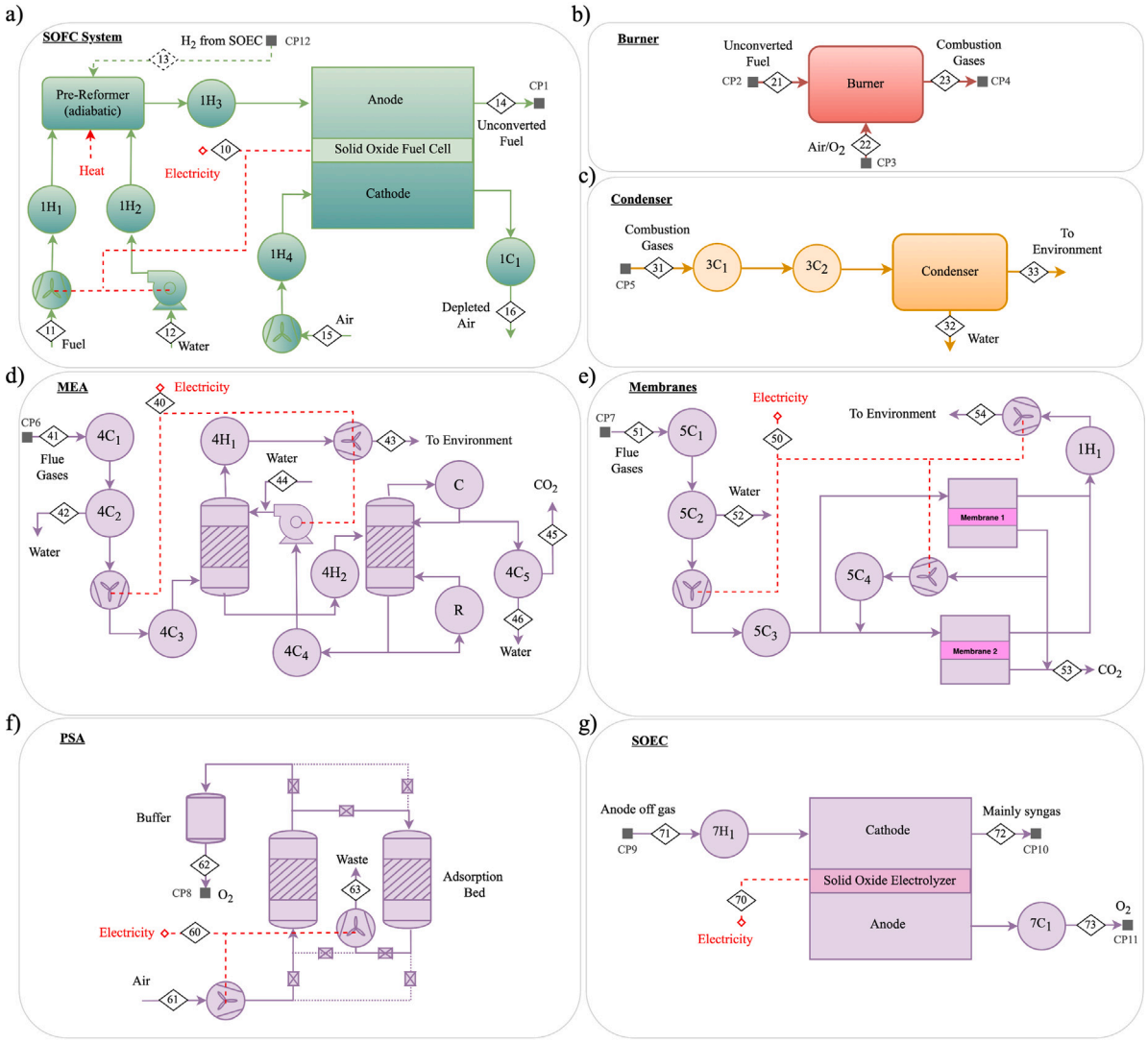

Fig. 3. Detailed system layouts for (a) SOFC system, (b) Burner, (c) Condenser, (d) MEA, (e) Membranes, (f) PSA and (g) SOEC; CP: connection point.

Aspen Plus to exchange decision variable values and retrieve key data from the process model. The heat cascade problem, formulated as a mixed integer linear programming (MILP) problem, is solved using the AMPL/CPLEX solver.

The integrated SOFC-SOEC system has been optimized to explore trade-off solutions among three conflicting objective functions, as listed in Table 3: minimizing external water flow rate, maximizing electrical efficiency, and maximizing the anode off-gas (AOG) recirculation fraction. Eq. (1) represents the electrical efficiency (η) of the SOFC system, defined as the ratio of the net electrical power output to the total energy input provided by the fuel. In this context, the term $\dot{m}_{fuel}$ represents the mass flow rate of the fuel, and LHV_{fuel} denotes the lower heating value of the fuel. P_{SOFC} refers to the electrical power generated by the SOFC stack, while P_{BOP} and P_{SOEC} accounts for the power consumed by the balance of plants (compressors, pumps, etc.) and SOEC stack, respectively.

$$\eta = \frac{P_{SOFC} - P_{BOP} - P_{SOEC}}{\dot{m}_{fuel} \cdot LHV_{fuel}} \quad (1)$$

Another objective function, the external water consumption, is directly tied to the scale of the water purification unit, with larger installations increasing system complexity and cost. The SOFC system can recirculate part of the AOG back to the external reformer via an AOG blower to reuse unreacted fuel and supply high-temperature steam. A higher AOG recirculation fraction improves the conversion of waste heat into chemical energy, reduces external water consumption, and decreases the heat demand of the external reformer. However, this may lower the system's electrical efficiency due to the power consumption of the AOG blower.

Regarding decision variables, the reforming temperature for the pre-reformer is maintained within a standard operational range, while the reforming fraction is determined by catalyst characteristics and operating parameters. Commercially available fuel cell stacks support internal reforming ratios of up to 0.9, leading to lower external reforming. The ranges for natural gas and external water usage are set based on specifications provided by the stack manufacturer [74]. Further, the SOEC power input, linked to the active SOEC stack area, is also defined as a decision variable to analyse its complex relationship with the overall system performance. Finally, several constraints have been implemented to meet industrial requirements. The steam-to-carbon and oxygen-to-carbon ratios are applied to prevent carbon deposition. Additionally, the O_2 mole fraction at the burner outlet is constrained to facilitate model convergence while maintaining the required CO_2 purity for capture. Overall, the multi-objective optimization framework is effectively able to explore the optimal system performance while adhering to industrial and operational constraints.

Table 2
Design and operating specifications of SOFC system, MEA, Membranes, PSA, and SOEC system (T - temperature, P - pressure, AOG - Anode off gas, * - after water condensation, A.C. - activated carbon, BSF - bed size factor).

SOFC system			
Stack area	−3 m^2	Reformer operating T	550 °C
Current density	0.4 A/cm^2	Reformer reforming fraction	0.3
Stack P drop	0.08 bar	Air blower suction P	1 bar
Stack T difference	70 °C	Air blower P increase	0.3 bar
Stack outlet T	750 °C	Air blower efficiency	0.8
Single pass fuel utilization	0.85	AOG blower maximum inlet T	120 °C
MEA			
Solvent	Monoethanolamine	Desorber heat/kg-CO_2	4.52 MJ
Absorber P	5 bar	Desorber P	1.62 bar
Absorber T	30 °C	Desorber T	120 °C
Membranes			
Type	PVam/PIP	Feed side P	5 bar
Permeance, CO_2	6500 GPU	Permeate side P	1 bar
Selectivity, CO_2/N_2	277	Total power/kg-CO_2	308.8 kJ
PSA			
Material	LiLSX	Adsorption P	2.25 bar
Selectivity, N_2/O_2	6.56	Desorption P	0.8125 bar
A.C. N_2 (0.79 bar, 20 °C)	0.93122 mmol/g	BSF, kg-material/(kg-O_2.h)	1.29
A.C. O_2 (0.21 bar, 20 °C)	0.03591 mmol/g	Total power/kg-O_2	2098.7 kJ
SOEC			
Stack inlet T	800 °C	Stack conversion efficiency	0.9
Stack outlet T	800 °C	Single-cell voltage	1.32 V

Table 3
Optimization problem formulation for novel SOFC-SOEC system.

Objective functions		
Minimization F1, mole/s	External water flow rate	
Maximization F2, %	Electrical efficiency	
Maximization F3, –	AOG recirculation fraction	
Decision Variables	**Minimum**	**Maximum**
Reforming temperature for pre-reformer X1, °C	510	550
Reforming ratio for pre-reformer X2, –	0.1	0.3
SOEC power input X3, kW	0.25	2.5
Natural gas flow rate X4, mole/s	0.0155	0.020
External water flow rate X5, mole/s	0.008	0.07
AOG recirculation ratio X6, –	0.00001	0.88
Constraints		
Steam to carbon (S/C) ratio, –	>1.5	
Oxygen to carbon (O/C) ratio, –	>2.5	
Burner downstream O_2 mole fraction, %	<2	

3.4. Techno-economic analysis assumptions

The techno-economic analysis methodology has been extensively detailed in previous studies [81,83,84]. Therefore, this study does not reiterate all the details. However, it is essential to outline the key assumptions that can influence the results.

The capital investment (CAPEX) for a process of size S is calculated using Eq. (2). In this equation, $CAPEX_{ref}$ represents the reference cost, S_{ref} is the reference size, α is the scaling factor, and $CEPCI_{2024}$ and $CEPCI_{ref}$ are the Chemical Engineering Plant Cost Indices (CEPCI) for the year 2024 and the reference year, respectively. The annualized investment cost is calculated using Eq. (3), with the annualization factor (AF), defined in Eq. (4), accounting for the interest rate (i) and the equipment lifetime (n), enabling the conversion of total capital cost into annualized values.

$$CAPEX(S)_{2024} = CAPEX_{ref} \cdot \left(\frac{S}{S_{ref}}\right)^{\alpha} \cdot \frac{CEPCI_{2024}}{CEPCI_{ref}} \quad [USD] \tag{2}$$

$$CAPEX(S)_{n,i} = CAPEX(S)_{2024} \cdot AF \quad [USD/y] \tag{3}$$

$$AF = \frac{i \cdot (1+i)^n}{(1+i)^n - 1} \tag{4}$$

Overall, CAPEX for each case has been estimated based on values reported in the literature or EU projects [64,72,74,84]. A plant operation time of 8000 h per year has been assumed. Since the capital cost data for the various processes are recent, the impact of the CEPCI has not been considered. For annualizing the capital cost, a lifetime of 10 years and an interest rate of 5% have been applied. The operating cost (OPEX) is calculated based on fuel consumption, water consumption, and the CO_2 tax on emissions. For Switzerland, the price of natural gas is 28 euro/MWh [85], deionized water costs 14.5 USD/t [86], and the CO_2 tax is 96 USD/t [87]. Furthermore, several other cost assumptions that are used for each module have been presented below.

For the shared modules, including the SOFC, burner, and condenser, the total cost is 10,000 USD/kW [88], with the SOFC contributing 74% of the cost, the burner 6%, and the condenser 12% [72]. The lifetime of the SOFC BoP (balance of plant), burner, and condenser is 10 years, while the SOFC stack has a lifetime of 5 years. The total cost includes a stack replacement after 5 years. In the future, the total cost is projected to decrease to 4000 USD/kW [89,90].

For post-combustion scenarios, in Case 1A, where MEA is applied, Nwaoha et al. [91] reported a capital cost of 29.8 million USD for a plant with a capacity of 774,775 t/y. Cost estimation assumes a scaling factor of 0.7 and a plant lifetime of 10 years. For Case 1B, where membranes are used, the system cost includes compressors, turbines, and membranes, with the membrane cost estimated at 500 USD/m^2 [92]. Compressor and turbine costs are derived using literature correlations [93]. The total cost also includes membrane replacement every two years, with an overall system lifetime of 10 years.

For oxy-combustion scenarios, in Case 2A, where PSA is applied, the total cost for a 101 Nm^3/h PSA unit is 392,700 USD, including compressors, air treatment, and adsorption beds [94]. Material replacement is required every five years, with a scaling factor of 0.7 and a plant lifetime of 10 years assumed for cost estimation. In Case 2B, when SOEC is used to supply oxygen, the maximum power received by the SOEC can be up to three times higher than the maximum power production in SOFC mode [79,89,90]. Therefore, the cost of the SOEC has been calculated as one-third of the SOFC cost.

4. Optimization of advanced SOFC-SOEC system

Fig. 4 illustrates the detailed process flow diagram of the proposed SOFC-SOEC system, designed to identify optimal operating conditions

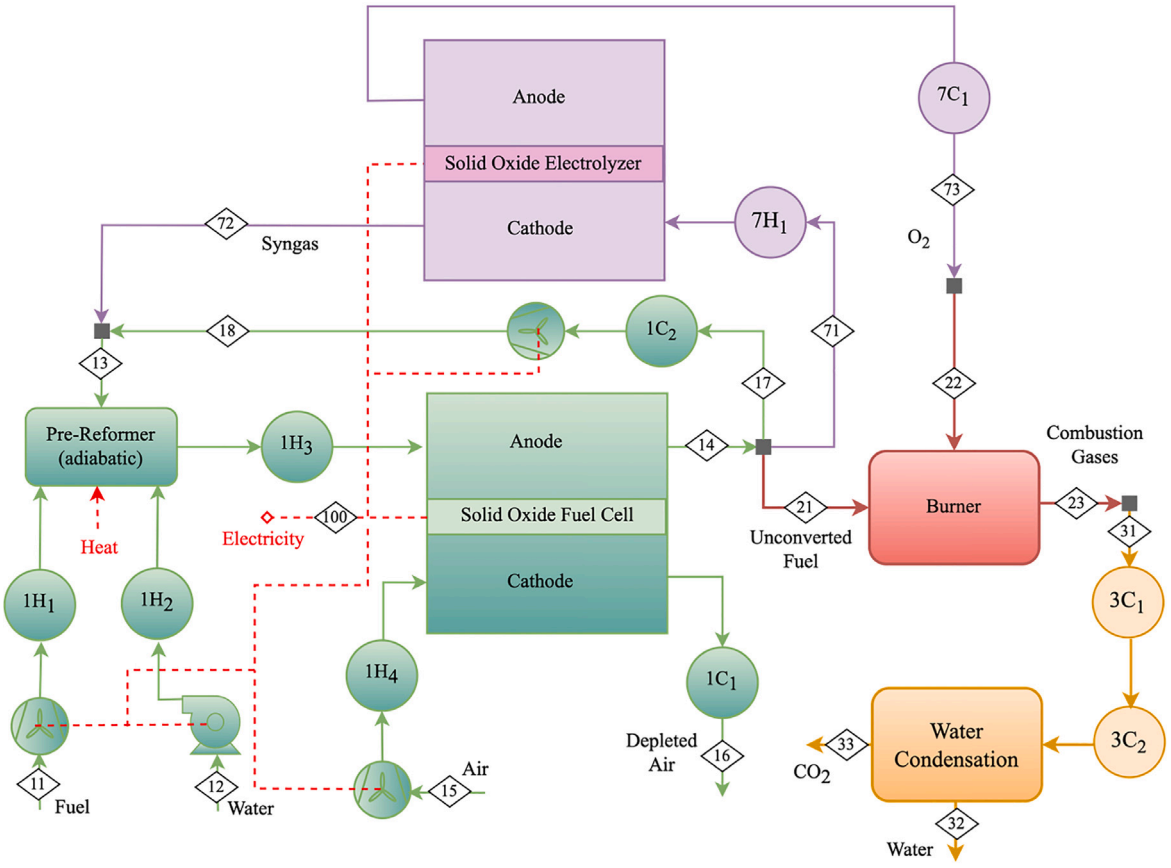

Fig. 4. Advanced SOFC-SOEC system with burner and water condenser/heat recovery.

for enhanced performance while adhering to industrial constraints. In this configuration, electricity is generated in the SOFC stack using fuel, and a portion of the anode off-gas is directed to the SOEC input, where O_2 and syngas are produced. Within the integrated SOFC-SOEC system, the electricity required for the co-electrolyzer is supplied directly by the fuel cell. The produced oxygen is used to complete the stoichiometric oxidation of unconverted fuel from the fuel cell, while the syngas are injected into the reformer, recovering part of the energy consumed by the electrolyzer. Detailed connections among different modules are also described in the methodology section.

A total of thirty-seven Pareto-optimal solutions were obtained, as illustrated in Fig. 5(a). From these, six representative Pareto-optimal solutions were selected for further analysis, as shown in Fig. 5(b). Generally, system electrical efficiency is inversely related to external water usage. Higher electrical efficiency requires increased external water usage and results in a lower AOG recirculation fraction. For the high-efficiency case, highlighted in blue colour, the system achieves an electrical efficiency of 61.5% with an external water flow of approximately 0.02 mol/s and an AOG recirculation of around 0.4. Additionally, about 0.4 kW of electricity is required by the SOEC stack to produce sufficient O_2, while the fuel input is 0.017 mol/s. It is important to note that a higher AOG recirculation does not necessarily lead to improved system efficiency, contrary to common assumptions that it reduces fresh fuel input. This is primarily due to the significant energy consumption of the AOG blower, which offsets the benefits of reduced energy input. For example, comparing the dark blue- and orange-shaded data sets reveals that increased AOG recirculation does not improve efficiency due to this effect. However, a higher AOG recirculation significantly decreases external water requirements, which can potentially decrease the size or cost of the water purification unit. This is evident when comparing the dark blue- and light blue-shaded data sets, where the external water requirement drops from 0.02 to 0.0081 mol/s.

In addition, comparing the yellow- and purple-shaded data sets reveals a clear pattern: a decrease in the external reforming fraction corresponds to improved system efficiency. Similarly, this principle applies to the external reforming temperature, as shown by the green- and blue-shaded data sets. A lower external reforming is preferred because the reforming reaction is endothermic, which increases internal reforming within the stack. This helps in balancing the heat within the stack, reducing the fresh air required for cooling and lowering the air blower power consumption, thereby improving system efficiency [40, 69].

In general, the proposed SOFC-SOEC system layout has the potential to reduce the total heat exchange area and external water consumption. Additionally, this section highlights the importance of system optimization in determining the optimal operating conditions, particularly for non-mature technologies. Before comparing such technologies with more established alternatives, it is essential to evaluate their performance under optimized conditions to ensure a fair and meaningful comparison.

4.1. Advantages and potential of SOFC-SOEC system

The proposed novel system initially considers SOFC and SOEC as separate components. However, the reversibility of solid oxide cells is well-established, enabling operation in both fuel cell and electrolyzer modes. Due to differences in voltage and current density, the electricity input required for SOEC is approximately three times the electricity output of SOFC. As a result, the active area required for SOEC is considerably smaller than that of SOFC in the integrated SOFC-SOEC system. For example, taking the best efficiency case after optimization, which has been used for technology comparisons in the later section, and is presented in Table 4, the active area of SOEC is estimated to be less than 1.3% of the SOFC active area. This integration results in a

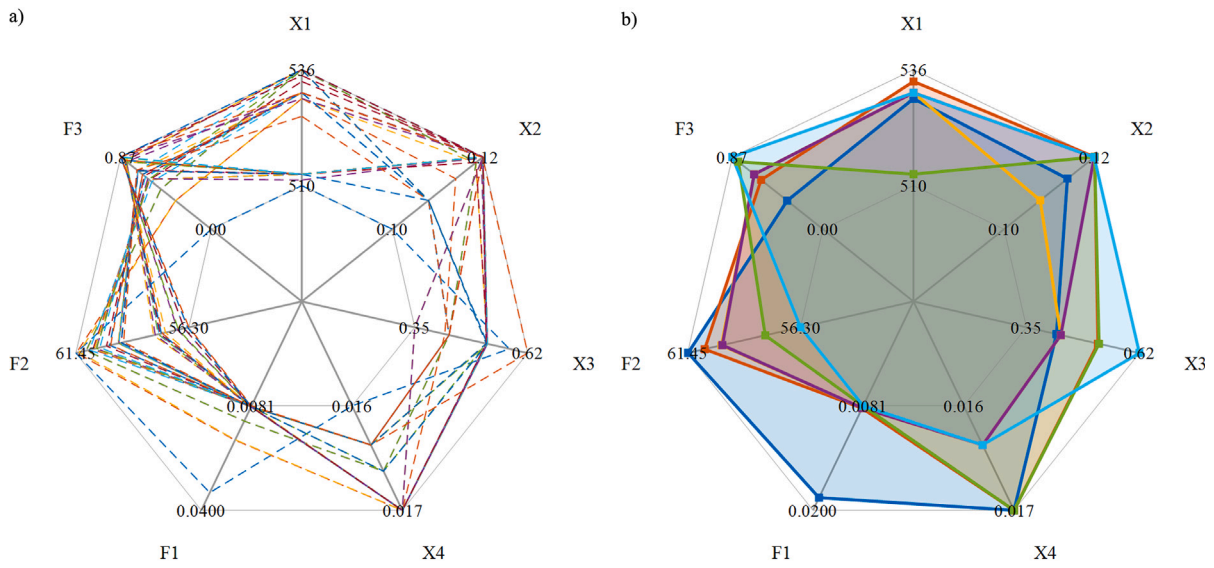

Fig. 5. Pareto-optimal solutions obtained for novel SOFC-SOEC system, (a) all 37 Pareto-optimal solutions, and (b) 6 selected Pareto-optimal solutions; F1: external water flow rate (mole/s), F2: electrical efficiency (%), F3: AOG recirculation, X1: reforming temperature for pre-reformer (°C), X2: reforming fraction for re-reformer, X3: SOEC power input (kW), X4: natural gas flow rate (mole/s).

highly compact system that follows modularity principles and avoids complex piping. A self-capturing CO_2 system offers a more compact and controllable solution compared to adding standalone CO_2 capture technologies.

Moreover, beyond power production, the SOFC-SOEC system offers the flexibility to transition into SOEC mode in scenarios where renewable electricity is readily available. This enables the generation of clean fuels through (co-)electrolysis, followed by fuel upgrading. A study by Haeun Shin et al. [95] highlights fuel production using excess renewable electricity and CO_2. This study expands on this by addressing the critical aspect of the CO_2 source, emphasizing the advantages of utilizing self-produced and captured CO_2. The reversible solid oxide cells (rSOC) considered in this study provide a closed-loop approach to energy storage and production. By utilizing carbon molecules (CH_4 and CO_2) within the system boundary, the rSOC system delivers a more self-contained and efficient solution.

5. Performance comparison for different systems

After optimizing the proposed SOFC-SOEC system (Case 2B), its performance is compared with other technologies. This section evaluates the performance of the Base Case, Case 1, and Case 2, using key performance indicators (KPIs) such as system electrical efficiency, CO_2 purity, and CO_2 recovery rate. Additionally, the heat potential for each case is analysed, considering options for directly delivering high-temperature heat externally or converting waste heat into electricity. Finally, a techno-economic analysis is presented to provide a comprehensive understanding of the strengths, weaknesses, market viability, and potential improvements for each technology.

5.1. Material flows and energetic performance

This study examines an SOFC stack generating approximately 10 kW of DC electricity using natural gas as the fuel. Table 4 summarizes the input and output flow rates for each subsystem, as depicted in Fig. 3. For post-combustion CO_2 capture processes, the CO_2 purity is approximately 98%. The MEA process (Case 1A) achieves a very high CO_2 recovery rate, consistent with findings in the literature that highlight MEA's efficiency in separating CO_2 from flue gases even with relatively low CO_2 concentrations [96]. Conversely, in the membrane process (Case 1B), 0.462 m^2 of the membrane is required, and it achieves a CO_2 recovery rate of 95%, with performance highly dependent on membrane selectivity and permeability [97]. For oxy-combustion cases (Case 2A and Case 2B), CO_2 recovery reaches 100%. However, in Case 2A, where PSA is applied, the product CO_2 contains N_2 impurities originating from the O_2 produced by PSA (94.4% CO_2 purity). In Case 2B, where SOEC is used, the product CO_2 is free from N_2 impurities.

A small portion of the electricity produced by the SOFC system is consumed by auxiliary units, such as pumps and compressors. In the Base Case, the natural gas compressor and water pump consume a minimal amount of electricity. The MEA process (Case 1A) requires additional electricity to compress the flue gases and increase the pressure of the MEA recycle stream. A small amount of electricity is recovered by a turbine before discharging the waste gas stream to the environment, resulting in a net electricity consumption of 0.19 kW. In the membrane system (Case 1B), electricity is required to compress the feed and permeate streams, while some electricity is recovered by expanding the waste stream. The net electricity consumption for this case is 0.24 kW. For the PSA process (Case 2A), electricity is consumed for air compression, while waste expansion generates some electricity, resulting in a net requirement of 0.282 kW. Finally, in the SOEC system (Case 2B), electricity is consumed to split part of the AOG into syngas and oxygen, leading to a higher net electricity consumption of 0.319 kW. All electrical connections are illustrated in Fig. 3, and Table 4 summarizes the electricity produced and consumed by different components in the Base Case, Case 1, and Case 2.

Overall, Cases 1A, 1B, and 2A achieve a net DC efficiency of approximately 65%, while Case 2B has a slightly lower net DC efficiency of about 62%. Although Case 2B demonstrates the lowest electrical efficiency among the cases, its performance remains comparable to the other three conventional technologies. This study considers captured CO_2 at 1 bar to standardize the comparison across all cases. The focus is not on optimizing CO_2 compression and storage; however, as an example, if CO_2 compression is considered, approximately 90 kWh/tCO_2 of electrical power is required to achieve the storage pressure around 150 bar. For the systems studied here, this translates to an estimated electricity consumption of around 0.25 kW, leading to a roughly 1.6% efficiency reduction. While exploring optimal CO_2 compression and storage, potentially linked to variation in the system's pressure, could be an interesting area of research, it is beyond the scope of this study [98]. Nevertheless, it is important to note that these conventional technologies had longer development timelines to

Table 4
Details of materials and electricity flows for Base Case: SOFC System + Burner + Condenser, Case 1A: SOFC System + MEA, Case 1B: SOFC System + Membranes, Case 2A: SOFC System + PSA + Burner + Condenser, and Case 2B: SOFC System + SOEC + Burner + Condenser. Stream numbers are shown in Fig. 3.

	Stream No	Base case	Case 1A	Case 1B	Case 2A	Case 2B optimized
SOFC system, mol/s	11	0.0185	0.0185	0.0185	0.0185	0.0166
	12	0.0400	0.0400	0.0400	0.0400	0.0336
	13	–	–	–	–	0.0014
	14	0.0955	0.0955	0.0955	0.0955	0.0850
	15	1.4680	1.4680	1.4680	1.4680	1.8510
	16	1.4350	1.4350	1.4350	1.4350	1.8180
Burner, mol/s	21	0.0955	0.0955	0.0955	0.0955	0.0850
	22	0.0200	0.0200	0.0200	0.0043	0.0006
	23	0.1120	0.1120	0.1120	0.0960	0.0850
Condenser, mol/s	31	0.1120			0.0960	0.0850
	32	0.0770			0.0770	0.0680
	33	0.0350			0.0190	0.0170
MEA, mol/s	41		0.1117			
	42		0.0759			
	43		0.0070			
	44		0.0163			
	45		0.0189			
	56		0.0076			
Membranes, mol/s	51			0.1117		
	52			0.0759		
	53			0.0180		
	54			0.0178		
PSA, mol/s	61				0.0768	
	62				0.0043	
	63				0.0725	
SOEC, mol/s	71					0.0014
	72					0.0014
	73					0.0006
Electricity consumption						
: MEA, kW	40		−0.19			
: Membranes, kW	50			−0.24		
: PSA, kW	60				−0.28	
: SOEC, kW	70					−0.32
Electricity production:						
: SOFC System, kW	10	9.90	9.90	9.90	9.90	9.13
: Net, kW	–	9.90	9.71	9.66	9.61	8.24
Fuel energy input, kW	–	14.84	14.84	14.84	14.84	13.30
Electrical efficiency, %	–	66.69	65.41	65.07	64.79	61.92
CO_2 purity, mol%	–	–	97.9	98.0	94.4	100
CO_2 recovery, % (wt./wt.)	–	–	99.8	95.0	100	100

reach their current level of maturity, which must be considered in such comparisons. Most importantly, Case 2B, which incorporates the SOFC-SOEC system, excels in terms of CO_2 purity and recovery. This advantage is particularly significant when accounting for the impurities commonly found in real-world natural gas sources.

5.2. Heat flows and heat valorization

As the SOFC system operates at high temperatures, it generates high-temperature heat as a co-product. This subsection explores two approaches for utilizing this heat. First, the system behaviour is analysed when the SOFC system co-generates high-temperature heat at 600 °C. Second, the Rankine cycle is integrated to convert waste heat into electricity, thereby improving the system's electrical efficiency. The results of both approaches are presented and discussed.

The Base Case and Case 2A each have eight hot and cold streams, while Case 2B has ten hot and cold streams. Additionally, Case 1A and Case 1B include fifteen and eleven hot and cold streams, respectively. Consequently, Case 1A should require the highest number of heat exchangers among all cases.

For each case, a heat cascade problem has been solved to determine the required amounts of hot and cold utilities [99]. The integrated systems for the Base Case, Case 1B, Case 2A, and Case 2B have sufficient heat available, requiring no hot utility to close the heat balance. In contrast, Case 1A requires a minimal amount of hot utility. Fig. 6 illustrates the grand composite curves for the different cases. The integrated system generates waste heat at very high temperatures, which can be utilized for industrial applications. Fig. 6 also shows grand composite curves with heat extraction at 600 °C. Table 5 summarizes the heat extracted or supplied for each case: 2.542 kW for the Base Case, 2 kW for Case 1A, 2.715 kW for Case 1B, 2.574 kW for Case 2A, and 2.787 kW for Case 2B. For Case 1A, high-temperature heat is unavailable due to blockage, necessitating the use of a low-temperature heat pump to supply high-temperature heat. The optimized heat pump operates between 50 and 150 °C [100] and consumes 0.984 kW of electricity. Overall, in Case 2B, the proposed SOFC-SOEC system delivers the maximum amount of heat, primarily due to its simplified plant layout, which requires fewer coolers and heaters, thereby enhancing system thermal performance.

The high-temperature waste heat available from the integrated system is also utilized to operate a Rankine cycle for electricity production. By using this concept, this subsection focuses on optimizing the integration of the Rankine cycle to maximize electricity production. For Case 1A, a heat pump operating between 50 and 150 °C is integrated with the Rankine cycle. The optimum pressure levels for the Rankine cycle in each design case are reported in Table 5 [101]. Among the cases, Case 1B (SOFC System + Membranes) achieves the highest additional electricity production, generating 1.952 kW using the Rankine cycle. Conversely, Case 1A (SOFC System + MEA) generates 0.835 kW net electricity, as the Rankine cycle produces 1.651 kW, but the heat pump consumes 0.816 kW of electricity. Fig. 7 illustrates integrated composite curves with the optimized Rankine cycle for different cases.

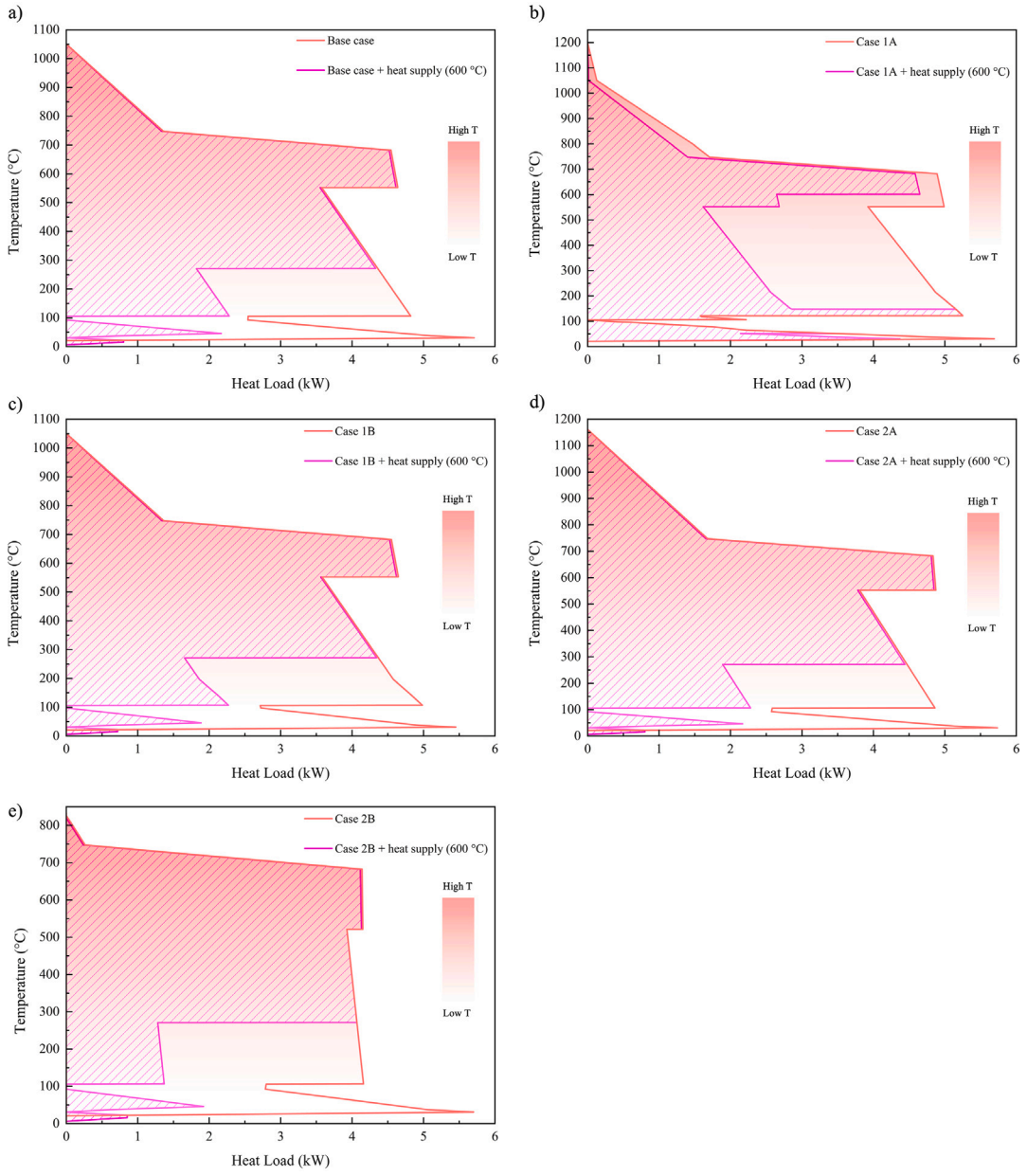

Fig. 6. Grand composite curves without/with industry heat supply (600 °C) for (a) Base case, (b) Case 1A, (c) Case 1B, (d) Case 2A, and (e) Case 2B.

The electricity produced from the Rankine cycle enhances the overall fuel-to-electricity conversion efficiency of the integrated system. The performance improvement from integrating the Rankine cycle is detailed in Table 5. The overall efficiency of the integrated clean power production system exceeds 75% for Cases 1B, 2A, and 2B, while Case 1A achieves an efficiency of approximately 70%.

5.3. Techno-economic analysis

In order to compute the electricity production cost for each case, the capital and operating costs have been evaluated in detail. This study considers a 10 kW power output from the integrated system. To ensure a fair comparison, the flow rates in Table 4 were adjusted by multiplication factors of 1.011, 1.030, 1.036, 1.040, and 1.214 for the Base Case (SOFC System + Burner + Condenser), Case 1A (SOFC System + Burner + MEA), Case 1B (SOFC System + Burner + Membranes), Case 2A (SOFC System + PSA + Burner + Condenser), and Case 2B (SOFC System + SOEC + Burner + Condenser), respectively, to normalize the data for consistent comparison.

The integrated system produces 10 kW of electricity, which is equivalent to 80,000 kWh of annual electricity production, assuming a plant operating time of 8000 h/y. Fig. 8(a) shows the values of CAPEX, OPEX, CO_2 tax, system electrical efficiency, electricity price, CO_2 purity and recovery, and CO_2 capture investment for different cases. Case 1A has the highest investment cost, amounting to 14,656 USD/y, while Case 1B, Case 2A, and Case 2B have comparable investment levels. As expected, the Base Case incurs the lowest cost since it does not include CO_2 capture equipment. However, it must pay the CO_2 tax of 2274 USD/y as presented in the third column of Fig. 8(a).

The operating costs for all four cases are comparable, ranging from 3854 to 4063 USD/y. Case 2B (SOFC System with SOEC) has a lower electrical efficiency but achieves high CO_2 purity and recovery. Case 1A, Case 1B, and Case 2A exhibit comparable electrical efficiencies; however, Case 1B and Case 2A achieve lower CO_2 purity and recovery, while Case 1A incurs high investment costs and generates less waste heat. Detailed cost analysis data is provided in Tables 6.

Table 5
Details of utilities and electricity flows for Base Case, Case 1A, Case 1B, Case 2A, and Case 2B (RC — Rankine Cycle, HP — Heat Pump, P — Pressure, SH — super-heating).

	Base case	Case 1A	Case 1B	Case 2A	Case 2B
Hot utility (1200 °C), kW	–	0.342	–	–	–
Cold utility (20–30 °C), kW	6.510	6.460	6.167	6.536	6.551
Heat supply at 600 °C, kW	2.542	2.000	2.715	2.574	2.787
Cold utility (20–30 °C), kW	3.167	5.136	2.729	3.161	2.911
Electricity consumption: HP (E_{HP1}), kW	–	0.984	–	–	–
Electricity production: RC (E_{RC}), kW	1.894	1.651	1.952	1.923	1.787
RC P level 1 (bar), SH (°C)	200, 200	200, 200	200, 200	200, 200	200, 200
P Level 2 (bar), SH (°C)	50, 100	50, 100	50, 100	50, 100	50, 100
P Level 3 (bar), SH (°C)	5, 10	5, 10	5, 10	5, 10	5, 10
P Level 4 (bar), SH (°C)	1.5, 10	1.5, 10	1.5, 10	1.5, 10	1.5, 10
P Level 5 (bar), SH (°C)	0.09, 1	–	0.09, 1	0.09, 1	0.09, 1
Hot utility (1200 °C), kW	–	0.035	–	–	–
Cold utility (20-30 °C), kW	4.661	5.362	4.260	4.659	4.806
Electricity consumption: HP (E_{HP2}), kW	–	0.816	–	–	–
Electricity production:					
Integrated system (E_{IS}), kW	9.896	9.706	9.656	9.614	8.235
Net ($E_{IS} + E_{RC} - E_{HP1} - E_{HP2}$), kW	11.790	10.373	11.608	11.537	10.022
Fuel energy input, kW	14.840	14.840	14.840	14.840	13.299
Electrical efficiency, %	79.45	69.90	78.22	77.74	75.36

Table 6
Details cost analysis data for Base Case, Case 1A, Case 1B, Case 2A, and Case 2B (RC — Rankine Cycle, HP — Heat Pump).

	Base Case	Case 1A	Case 1B	Case 2A	Case 2B
SOFC (current), $	74 000	74 000	74 000	74 000	74 000
SOFC (future), $	3418	3418	3418	3418	3418
Burner, $	6000	6000	6000	6000	6000
Condenser, $	12 000	12 000	12 000	12 000	12 000
MEA, $		21 167			
MEM, $			6362		
PSA, $				7604	
SOEC (current), $					7881
SOEC (future), $					364
CAPEX (current), $/y	11 914	14 656	12 738	12 899	12 935
CAPEX (future), $/y	2774	5515	3598	3758	2821
OPEX, $/y	6054	3854	3991	3890	4063
Fuel flow, mol/s	0.01869	0.01906	0.01916	0.01924	0.02013
Water flow, mol/s	0.04042	0.04121	0.04143	0.04161	0.04249
CO_2 flow to environment, mol/s	0.01869	0	0.00096	0	0
Fuel cost, $/y	3476	3544	3562	3578	3743
Water cost, $/y	304	310	311	313	319
CO_2 tax, $/y	2274	0	117	0	0
Electrical efficiency, %	66.69	65.41	65.07	64.79	61.92
Electrical efficiency with RC and HP, %	79.45	69.9	78.22	77.74	75.36
Electricity prices (current), $/kWh	0.225	0.231	0.209	0.21	0.212
Electricity prices (future), $/kWh	0.11	0.117	0.095	0.096	0.086
Electricity prices with RC and HP (current), $/kWh	0.1885	0.2165	0.174	0.1749	0.1746
Electricity prices with RC and HP (future), $/kWh	0.0926	0.1096	0.0789	0.0797	0.0707
CO_2 purity, %	0	97.9	98	94.4	100
CO_2 captured percentage, %	0	99.8	95	100	100
CO_2 captured, kg/y	0	24 100	23 209	23 641	26 160
CO_2 capture investment (current), $/y	0	2741	824	985	1021
CO_2 capture investment (future), $/y	0	2741	824	985	47

However, cost estimations for developing technologies must be approached cautiously. In the context of reversible solid oxide cell (rSOC) technology, ongoing efforts aim to optimize its manufacturing process. These efforts focus on factors that are expected to influence the technology's development trajectory, such as improvements in materials for increased efficiency, potential joint ventures among international manufacturing companies, and an expected increase in production volume due to rising demand. As these advancements materialize over time, the cost of SOFC technology is expected to decrease, making it more competitive in the future. Thus, the future market status of SOFC technologies is an interesting area that has also been explored.

Fig. 8(b) illustrates the results by incorporating future rSOC cost projections; the findings highlight the significant implications of projected rSOC cost reductions. For instance, a production volume of 50,000 units per year is projected to lower the annual cost of a 10 kW stack to 3418 USD [89,102]. As expected, the forecasted cost reductions led to a more than 50% decrease in CAPEX across all design cases.

Especially for Case 2B, the investment cost associated with CO_2 capture decreases to 47 USD/y for a 10 kW system. This reduction is primarily due to the high power density of the SOEC, as previously explained. The power input capacity of the SOEC is three times greater than the power output of the SOFC for the same electrolyte surface area, resulting in a lower investment cost for the SOEC, particularly as the cost of SOFC decreases. Furthermore, the economic advantage is amplified by the shared utilization of the common rSOC unit. In exchange for a marginal reduction in electrical efficiency, incorporating the projected future cost of rSOC technology enables an attainable electricity price of 0.086 USD/kWh in Case 2B. This case also achieves

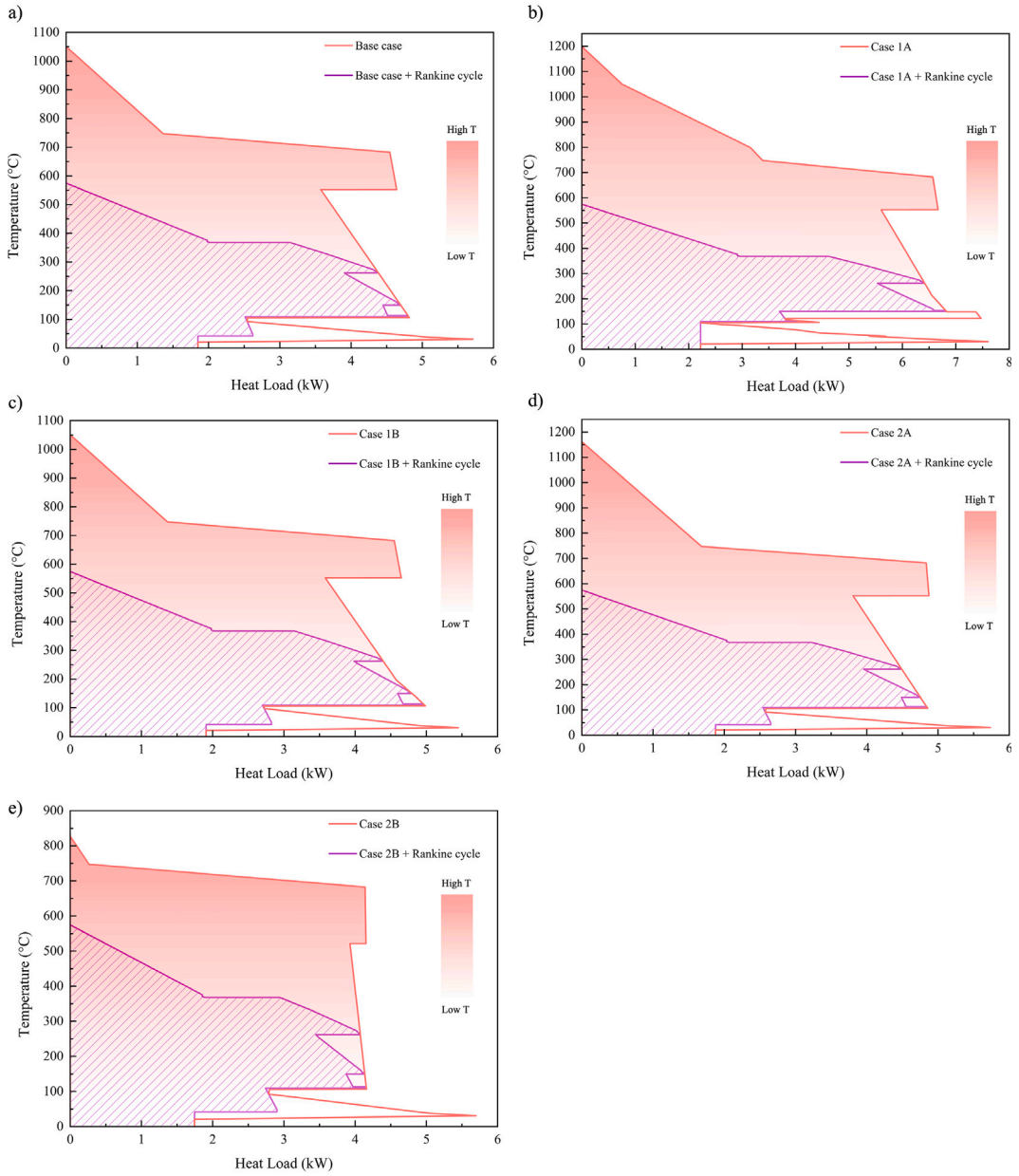

Fig. 7. Integrated composite curves with optimized Rankine cycle for (a) Base case, (b) Case 1A, (c) Case 1B, (d) Case 2A, and (e) Case 2B.

the highest levels of CO_2 purity and capture rate, which are critical factors. This advantage is especially significant given the practical consideration of impurities in natural gas in industrial settings, which could potentially reduce CO_2 purity across all scenarios.

5.4. General discussion on SOFC-SOEC system

The evaluation of the SOFC-SOEC system via KPIs provides valuable insights into its operational efficacy. This system uniquely integrates the SOFC with the SOEC, using part of the electricity produced by the SOFC in SOEC to produce oxygen. Despite this integration slightly reducing the overall system efficiency compared to other technologies, it remains competitively viable. A notable concern is the impact of slight efficiency reduction on the system's overall effectiveness and its suitability for large-scale adoption. However, exceptional CO_2 purity is the remarkable feature of this system, critical for processes like co-electrolysis or methanation where impurities severely affect both system efficiency and product quality [103].

The SOFC-SOEC system benefits from a unified plant layout and the use of a common stack, which supports a compact and streamlined design. This system design reduces the number of heat exchangers, simplifying the configuration and enabling a switch between fuel cell and electrolyzer modes within ten minutes [72]. Furthermore, compared to other fuel cell types, the SOFC offers multifunctionality, notably as a combined heat and power plant. This simplicity, cost-effectiveness, and promising system efficiency position the SOFC-SOEC technology as a competitive and flexible solution for future energy systems.

Cost considerations are critical for emerging technologies. Projections are inherently uncertain and closely linked to future technological advancements. For instance, an increase in production volumes could occur once the technology is proven to be viable [104,105]. The scalability of rSOC technology must also take into account its potential

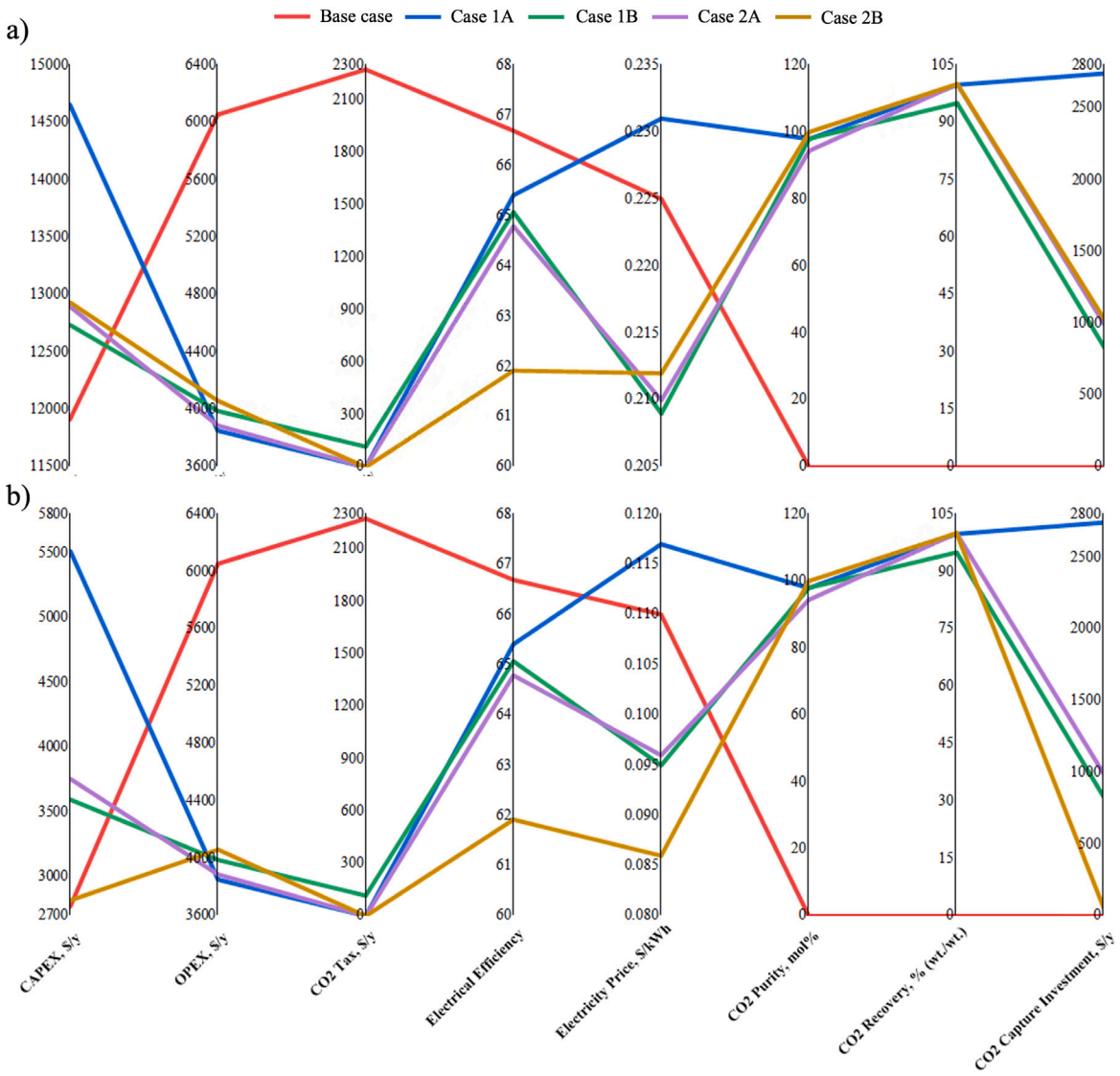

Fig. 8. Performance comparison for Base Case, Case 1A, Case1B, Case2A and Case 2B, based on 10 kW integrated system: (a) use of current cost for SOFC technology, (b) use of future cost for SOFC technology.

for long-term energy storage, which is especially important in regions experiencing intermittent renewable energy supply.

6. Conclusions

In this study, an innovative SOFC-SOEC system for clean power production with 100% CO_2 capture and purity has been proposed, developed, and thoroughly analysed. The results demonstrate that the SOFC-SOEC configuration achieves an impressive CO_2 purity, with system electrical efficiency reaching 62% and 75.4%, respectively, with and without heat valorization. Further, a comparative analysis of four distinct SOFC system configurations with CO_2 capture technologies was conducted. The findings highlight the superior performance of the SOFC-SOEC system compared to conventional technologies: membrane separation, which exhibits a lower CO_2 capture rate; pressure swing adsorption, which results in decreased purity; and amine absorption, which requires a more substantial investment and offers lower heat potential. The computed active area of the SOEC, a mere 1.3% of the SOFC active area, indicates that only a small portion of the electricity generated by the SOFC is diverted to SOEC operation. Moreover, through techno-economic analysis, it is demonstrated that the SOFC-SOEC system can achieve an electricity production cost as low as 0.085 USD/kWh, achievable by reducing the cost of the SOFC stack or by extending its operational lifetime in light of technological advancements. This study reveals significant potential by extensively exploring the integration of the SOFC-SOEC system for power generation with CO_2 capture. Ultimately, this innovative approach provides a pathway towards developing a more compact, flexible, and cost-effective clean power generation system.

Future studies should explore the dynamic optimization of the SOFC-SOEC system for enhanced adaptability to fluctuating demands. Economic analyses need to consider different locations and potential revenues from CO_2 utilization, such as fuel synthesis. Additionally, integrating renewable energy sources with SOFC-SOEC systems is crucial for ensuring compatibility with intermittent energy inputs and optimizing their deployment in sustainable energy frameworks. Considering the reversible mode of SOFC, which can convert captured CO_2 and renewable energy into stored fuel via co-electrolysis followed by fuel synthesis, the proposed system also emerges as a viable long-term strategy for mitigating global warming and addressing energy storage challenges.

CRediT authorship contribution statement

Xinyi Wei: Conceptualization, Methodology, Software, Validation, Writing – original draft. **Shivom Sharma:** Conceptualization, Methodology, Software, Validation, Writing – original draft. **Jan Van herle:** Conceptualization, Writing – review & editing, Supervision. **François Maréchal:** Conceptualization, Writing – review & editing, Supervision.

Declaration of competing interest

The authors declare that they have no known competing financial interests or personal relationships that could have appeared to influence the work reported in this paper.

Acknowledgments

The authors would like to acknowledge research funding from Fuel Cell Innovations, South Korea.

Data availability

Data will be made available on request.

References

[1] Liu L, He G, Wu M, Liu G, Zhang H, Chen Y, Shen J, Li S. Climate change impacts on planned supply–demand match in global wind and solar energy systems. Nat Energy 2023;8(8):870–80. http://dx.doi.org/10.1038/s41560-023-01304-w, URL https://www.nature.com/articles/s41560-023-01304-w.

[2] Molla S, Farrok O, Alam MJ. Electrical energy and the environment: Prospects and upcoming challenges of the World's top leading countries. Renew Sustain Energy Rev 2024;191:114177. http://dx.doi.org/10.1016/j.rser.2023.114177, URL https://linkinghub.elsevier.com/retrieve/pii/S1364032123010353.

[3] IEA I. IEA 50. 2023, URL https://www.iea.org/reports/coal-2023/.

[4] Roser HRaM. Energy Production and Consumption. 2020, URL https://ourworldindata.org/energy-production-consumption.

[5] Lacis AA, Schmidt GA, Rind D, Ruedy RA. Atmospheric CO_2 : Principal control Knob governing Earth's temperature. Science 2010;330(6002):356–9. http://dx.doi.org/10.1126/science.1190653, URL https://www.science.org/doi/10.1126/science.1190653.

[6] Lelieveld J, Klingmüller K, Pozzer A, Burnett RT, Haines A, Ramanathan V. Effects of fossil fuel and total anthropogenic emission removal on public health and climate. Proc Natl Acad Sci 2019;116(15):7192–7. http://dx.doi.org/10.1073/pnas.1819989116, URL https://pnas.org/doi/full/10.1073/pnas.1819989116.

[7] Do TN, You C, Kim J. A CO_2 utilization framework for liquid fuels and chemical production: techno-economic and environmental analysis. Energy Environ Sci 2022;15(1):169–84. http://dx.doi.org/10.1039/D1EE01444G, URL http://xlink.rsc.org/?DOI=D1EE01444G.

[8] Navarro J, Baena-Moreno F, Centeno M, Laguna O, Almagro J, Odriozola J. Process design and utilisation strategy for CO2 capture in flue gases. Technical assessment and preliminary economic approach for steel mills. Renew Sustain Energy Rev 2023;184:113537. http://dx.doi.org/10.1016/j.rser.2023.113537, URL https://linkinghub.elsevier.com/retrieve/pii/S1364032123003945.

[9] Yang S, Gao HO, You F. Model predictive control for distributed energy systems management in electrifying buildings: carbon emission reduction in response to dynamic electricity price and carbon intensity. In: 2023 American control conference. ACC, San Diego, CA, USA: IEEE; 2023, p. 3797–802. http://dx.doi.org/10.23919/ACC55779.2023.10156632, URL https://ieeexplore.ieee.org/document/10156632/.

[10] Pashchenko D. Hydrogen-rich gas as a fuel for the gas turbines: A pathway to lower CO2 emission. Renew Sustain Energy Rev 2023;173:113117. http://dx.doi.org/10.1016/j.rser.2022.113117, URL https://linkinghub.elsevier.com/retrieve/pii/S1364032122009984.

[11] Will F. Fuel conservation and emission reduction through novel waste heat recovery for internal combustion engines. Fuel 2012;102:247–55. http://dx.doi.org/10.1016/j.fuel.2012.06.044, URL https://linkinghub.elsevier.com/retrieve/pii/S0016236112004644.

[12] Vilas Boas FM, Borges-da Silva LE, Villa-Nova HF, Bonaldi EL, Oliveira LEL, Lambert-Torres G, Assuncao Fd, Costa CId, Campos MM, Sant'Ana WC, Lacerda J, da Silva Junior JLM, da Silva EG. Condition monitoring of internal combustion engines in thermal power plants based on control charts and adapted nelson rules. Energies 2021;14(16):4924. http://dx.doi.org/10.3390/en14164924, URL https://www.mdpi.com/1996-1073/14/16/4924.

[13] Fu L, Zhao X, Zhang S, Li Y, Jiang Y, Li H, Sun Z. Performance study of an innovative natural gas CHP system. Energy Convers Manage 2011;52(1):321–8. http://dx.doi.org/10.1016/j.enconman.2010.07.003, URL https://linkinghub.elsevier.com/retrieve/pii/S0196890410002955.

[14] Diangelakis NA, Panos C, Pistikopoulos EN. Design optimization of an internal combustion engine powered CHP system for residential scale application. Comput Manag Sci 2014;11(3):237–66. http://dx.doi.org/10.1007/s10287-014-0212-z, URL http://link.springer.com/10.1007/s10287-014-0212-z.

[15] Bidini G, Desideri U, Saetta S, Bocchini PP. Internal combustion engine combined heat and power plants: Case study of the University of Perugia power plant. Appl Therm Eng 1998;18(6):401–12. http://dx.doi.org/10.1016/S1359-4311(97)00051-3, URL https://linkinghub.elsevier.com/retrieve/pii/S1359431197000513.

[16] Szwaja M, Chwist M, Szymanek A, Szwaja S. Pyrolysis oil blended n-butanol as a fuel for power generation by an internal combustion engine. Energy 2022;261:125339. http://dx.doi.org/10.1016/j.energy.2022.125339, URL https://linkinghub.elsevier.com/retrieve/pii/S0360544222022228.

[17] Abdel-Rahman AA. On the emissions from internal-combustion engines:a review. Int J Energy Res 1998;22(6):483–513. http://dx.doi.org/10.1002/(SICI)1099-114X(199805)22:6<483::AID-ER377>3.0.CO;2-Z, URL https://onlinelibrary.wiley.com/doi/10.1002/(SICI)1099-114X(199805)22:6<483::AID-ER377>3.0.CO;2-Z.

[18] Heffel J. NOx emission reduction in a hydrogen fueled internal combustion engine at 3000 rpm using exhaust gas recirculation. Int J Hydrog Energy 2003;28(11):1285–92. http://dx.doi.org/10.1016/S0360-3199(02)00289-6, URL https://linkinghub.elsevier.com/retrieve/pii/S0360319902002896.

[19] Leach F, Kalghatgi G, Stone R, Miles P. The scope for improving the efficiency and environmental impact of internal combustion engines. Transp Eng 2020;1:100005. http://dx.doi.org/10.1016/j.treng.2020.100005, URL https://linkinghub.elsevier.com/retrieve/pii/S2666691X20300063.

[20] Braga LB, Silveira JL, Evaristo da Silva M, Machin EB, Pedroso DT, Tuna CE. Comparative analysis between a PEM fuel cell and an internal combustion engine driving an electricity generator: Technical, economical and ecological aspects. Appl Therm Eng 2014;63(1):354–61. http://dx.doi.org/10.1016/j.applthermaleng.2013.10.053, URL https://linkinghub.elsevier.com/retrieve/pii/S1359431113007722.

[21] Heppenstall T. Advanced gas turbine cycles for power generation: a critical review. Appl Therm Eng 1998;18(9–10):837–46. http://dx.doi.org/10.1016/S1359-4311(97)00116-6, URL https://linkinghub.elsevier.com/retrieve/pii/S1359431197001166.

[22] Rist JF, Dias MF, Palman M, Zelazo D, Cukurel B. Economic dispatch of a single micro-gas turbine under CHP operation. Appl Energy 2017;200:1–18. http://dx.doi.org/10.1016/j.apenergy.2017.05.064, URL https://linkinghub.elsevier.com/retrieve/pii/S0306261917305585.

[23] Pilavachi P. Power generation with gas turbine systems and combined heat and power. Appl Therm Eng 2000;20(15–16):1421–9. http://dx.doi.org/10.1016/S1359-4311(00)00016-8, URL https://linkinghub.elsevier.com/retrieve/pii/S1359431100000168.

[24] Baakeem SS, Orfi J, Al-Ansary H. Performance improvement of gas turbine power plants by utilizing turbine inlet air-cooling (TIAC) technologies in Riyadh, Saudi Arabia. Appl Therm Eng 2018;138:417–32. http://dx.doi.org/10.1016/j.applthermaleng.2018.04.018, URL https://linkinghub.elsevier.com/retrieve/pii/S1359431117367248.

[25] Luo Y, Liu Z, Luo S, Yuan X. Thermodynamic analysis of non-isothermal mixing's influence on the energy target of water-using networks. Comput Chem Eng 2014;61:1–8. http://dx.doi.org/10.1016/j.compchemeng.2013.10.008, URL https://linkinghub.elsevier.com/retrieve/pii/S009813541300330X.

[26] Polyzakis A, Koroneos C, Xydis G. Optimum gas turbine cycle for combined cycle power plant. Energy Convers Manage 2008;49(4):551–63. http://dx.doi.org/10.1016/j.enconman.2007.08.002, URL https://linkinghub.elsevier.com/retrieve/pii/S0196890407002828.

[27] Ersayin E, Ozgener L. Performance analysis of combined cycle power plants: A case study. Renew Sustain Energy Rev 2015;43:832–42. http://dx.doi.org/10.1016/j.rser.2014.11.082, URL https://linkinghub.elsevier.com/retrieve/pii/S1364032114010211.

[28] Zhang G, Zheng J, Yang Y, Liu W. A novel LNG cryogenic energy utilization method for inlet air cooling to improve the performance of combined cycle. Appl Energy 2016;179:638–49. http://dx.doi.org/10.1016/j.apenergy.2016.07.035, URL https://linkinghub.elsevier.com/retrieve/pii/S030626191630976X.

[29] Ol'khovskii GG. Combined cycle plants: Yesterday, today, and tomorrow (review). Therm Eng 2016;63(7):488–94. http://dx.doi.org/10.1134/S0040601516070041, URL http://link.springer.com/10.1134/S0040601516070041.

[30] Li Y, Zhang G, Bai Z, Song X, Wang L, Yang Y. Backpressure adjustable gas turbine combined cycle: A method to improve part-load efficiency. Energy Convers Manage 2018;174:739–54. http://dx.doi.org/10.1016/j.enconman.2018.07.077, URL https://linkinghub.elsevier.com/retrieve/pii/S0196890418308124.

[31] Barelli L, Ottaviano A. Supercharged gas turbine combined cycle: An improvement in plant flexibility and efficiency. Energy 2015;81:615–26. http://dx.doi.org/10.1016/j.energy.2015.01.004, URL https://linkinghub.elsevier.com/retrieve/pii/S0360544215000110.

[32] Zhao Y, Hagi H, Delahaye B, Maréchal F. A holistic approach to refinery decarbonization based on atomic, energy and exergy flow analysis. Energy 2024;296:131117. http://dx.doi.org/10.1016/j.energy.2024.131117, URL https://linkinghub.elsevier.com/retrieve/pii/S0360544224008892.

[33] Fajardy M, Morris J, Gurgel A, Herzog H, Mac Dowell N, Paltsev S. The economics of bioenergy with carbon capture and storage (BECCS) deployment in a 1.5 ° C or 2 ° C world. Global Environ Change 2021;68:102262. http://dx.doi.org/10.1016/j.gloenvcha.2021.102262, URL https://linkinghub.elsevier.com/retrieve/pii/S0959378021000418.

[34] Silveira BHM, Costa HKM, Santos EM. Bioenergy with carbon capture and storage (BECCS) in Brazil: A review. Energies 2023;16(4):2021. http://dx.doi.org/10.3390/en16042021, URL https://www.mdpi.com/1996-1073/16/4/2021.

[35] Wen D, Aziz M. Techno-economic analyses of power-to-ammonia-to-power and biomass-to-ammonia-to-power pathways for carbon neutrality scenario. Appl Energy 2022;319:119272. http://dx.doi.org/10.1016/j.apenergy.2022.119272, URL https://linkinghub.elsevier.com/retrieve/pii/S0306261922006298.

[36] Sharma S, Maréchal F. Design and optimization of membrane system for gas separation. In: Computer aided chemical engineering. Vol. 51, Elsevier; 2022, p. 865–70. http://dx.doi.org/10.1016/B978-0-323-95879-0.50145-4, URL https://linkinghub.elsevier.com/retrieve/pii/B9780323958790501454.

[37] Wang Z, Fan W, Zhang G. Comparison of the exergy efficiency of four power generation systems from methane using fuel cells. RSC Adv 2017;7(62):39391–402. http://dx.doi.org/10.1039/C7RA05245F, URL http://xlink.rsc.org/?DOI=C7RA05245F.

[38] Tsipis E, Agarkov D, Borisov Y, Kiseleva S, Tarasenko A, Bredikhin S, Kharton V. Waste gas utilization potential for solid oxide fuel cells: A brief review. Renew Sustain Energy Rev 2023;188:113880. http://dx.doi.org/10.1016/j.rser.2023.113880, URL https://linkinghub.elsevier.com/retrieve/pii/S1364032123007384.

[39] Wang L, Chen M, Küngas R, Lin T-E, Diethelm S, Maréchal F, Van Herle J. Power-to-fuels via solid-oxide electrolyzer: Operating window and techno-economics. Renew Sustain Energy Rev 2019;110:174–87. http://dx.doi.org/10.1016/j.rser.2019.04.071, URL https://linkinghub.elsevier.com/retrieve/pii/S1364032119302928.

[40] Wei X, Sharma S, Van Herle J, Maréchal F. Analysis and optimization of solid oxide fuel cell system with anode and cathode off gas recirculation. Renew Sustain Energy Rev 2025;208:115015. http://dx.doi.org/10.1016/j.rser.2024.115015, URL https://linkinghub.elsevier.com/retrieve/pii/S136403212400741X.

[41] Sgouridis S, Carbajales-Dale M, Csala D, Chiesa M, Bardi U. Comparative net energy analysis of renewable electricity and carbon capture and storage. Nat Energy 2019;4(6):456–65. http://dx.doi.org/10.1038/s41560-019-0365-7, URL https://www.nature.com/articles/s41560-019-0365-7.

[42] Oyenekan BA, Rochelle GT. Alternative stripper configurations for CO2 capture by aqueous amines. AIChE J 2007;53(12):3144–54. http://dx.doi.org/10.1002/aic.11316, URL https://onlinelibrary.wiley.com/doi/10.1002/aic.11316.

[43] Luis P. Use of monoethanolamine (MEA) for CO 2 capture in a global scenario: Consequences and alternatives. Desalination 2016;380:93–9. http://dx.doi.org/10.1016/j.desal.2015.08.004, URL https://linkinghub.elsevier.com/retrieve/pii/S001191641500418X.

[44] Meng F, Meng Y, Ju T, Han S, Lin L, Jiang J. Research progress of aqueous amine solution for CO2 capture: A review. Renew Sustain Energy Rev 2022;168:112902. http://dx.doi.org/10.1016/j.rser.2022.112902, URL https://linkinghub.elsevier.com/retrieve/pii/S1364032122007845.

[45] Wang L, Zhang Y, Wang R, Li Q, Zhang S, Li M, Liu J, Chen B. Advanced monoethanolamine absorption using sulfolane as a phase splitter for CO_2 capture. Environ Sci Technol 2018;52(24):14556–63. http://dx.doi.org/10.1021/acs.est.8b05654, URL https://pubs.acs.org/doi/10.1021/acs.est.8b05654.

[46] Zhao Y, Bian Y, Li H, Guo H, Shen S, Han J, Guo D. A comparative study of aqueous potassium lysinate and aqueous monoethanolamine for post-combustion CO $_2$ capture. Energy Fuels 2017;31(12):14033–44. http://dx.doi.org/10.1021/acs.energyfuels.7b02800, URL https://pubs.acs.org/doi/10.1021/acs.energyfuels.7b02800.

[47] Zoannou K-S, Sapsford DJ, Griffiths AJ. Thermal degradation of monoethanolamine and its effect on CO2 capture capacity. Int J Greenh Gas Control 2013;17:423–30. http://dx.doi.org/10.1016/j.ijggc.2013.05.026, URL https://linkinghub.elsevier.com/retrieve/pii/S1750583613002429.

[48] Ye C, Dang M, Yao C, Chen G, Yuan Q. Process analysis on CO2 absorption by monoethanolamine solutions in microchannel reactors. Chem Eng J 2013;225:120–7. http://dx.doi.org/10.1016/j.cej.2013.03.053, URL https://linkinghub.elsevier.com/retrieve/pii/S1385894713003781.

[49] Li K, Leigh W, Feron P, Yu H, Tade M. Systematic study of aqueous monoethanolamine (MEA)-based CO2 capture process: Techno-economic assessment of the MEA process and its improvements. Appl Energy 2016;165:648–59. http://dx.doi.org/10.1016/j.apenergy.2015.12.109, URL https://linkinghub.elsevier.com/retrieve/pii/S0306261915016827.

[50] Chawla M, Saulat H, Masood Khan M, Mahmood Khan M, Rafiq S, Cheng L, Iqbal T, Rasheed MI, Farooq MZ, Saeed M, Ahmad NM, Khan Niazi MB, Saqib S, Jamil F, Mukhtar A, Muhammad N. Membranes for CO $_2$ /CH $_4$ and CO $_2$ /N $_2$ gas separation. Chem Eng Technol 2020;43(2):184–99. http://dx.doi.org/10.1002/ceat.201900375, URL https://onlinelibrary.wiley.com/doi/10.1002/ceat.201900375.

[51] Wall Y, Braun G, Kaltenborn N, Voigt I, Brunner G. Separation of CO2/N2 by means of a carbon membrane. Chem Eng Technol 2012;35(3):508–12. http://dx.doi.org/10.1002/ceat.201100433, URL https://onlinelibrary.wiley.com/doi/10.1002/ceat.201100433.

[52] Idris A, Man Z, Maulud A, Khan M. Effects of phase separation behavior on morphology and performance of polycarbonate membranes. Membranes 2017;7(2):21. http://dx.doi.org/10.3390/membranes7020021, URL https://www.mdpi.com/2077-0375/7/2/21.

[53] Yousef S, Šereika J, Tonkonogovas A, Hashem T, Mohamed A. CO2/CH4, CO2/N2 and CO2/H2 selectivity performance of PES membranes under high pressure and temperature for biogas upgrading systems. Environ Technol Innov 2021;21:101339. http://dx.doi.org/10.1016/j.eti.2020.101339, URL https://linkinghub.elsevier.com/retrieve/pii/S2352186420316394.

[54] Cecopierigomez M, Palaciosalquisira J, Dominguez J. On the limits of gas separation in CO2/CH4, N2/CH4 and CO2/N2 binary mixtures using polyimide membranes. J Membr Sci 2007;293(1–2):53–65. http://dx.doi.org/10.1016/j.memsci.2007.01.034, URL https://linkinghub.elsevier.com/retrieve/pii/S0376738807000865.

[55] Liu J, Hou X, Park HB, Lin H. High-performance polymers for membrane CO $_2$ /N $_2$ separation. Chem Eur J 2016;22(45):15980–90. http://dx.doi.org/10.1002/chem.201603002, URL https://onlinelibrary.wiley.com/doi/10.1002/chem.201603002.

[56] Karousos DS, Lei L, Lindbr˚ athen A, Sapalidis AA, Kouvelos EP, He X, Favvas EP. Cellulose-based carbon hollow fiber membranes for high-pressure mixed gas separations of CO2/CH4 and CO2/N2. Sep Purif Technol 2020;253:117473. http://dx.doi.org/10.1016/j.seppur.2020.117473, URL https://linkinghub.elsevier.com/retrieve/pii/S138358662031947X.

[57] Jindaratsamee P, Ito A, Komuro S, Shimoyama Y. Separation of CO2 from the CO2/N2 mixed gas through ionic liquid membranes at the high feed concentration. J Membr Sci 2012;423–424:27–32. http://dx.doi.org/10.1016/j.memsci.2012.07.012, URL https://linkinghub.elsevier.com/retrieve/pii/S0376738812005492.

[58] Powell CE, Qiao GG. Polymeric CO2/N2 gas separation membranes for the capture of carbon dioxide from power plant flue gases. J Membr Sci 2006;279(1–2):1–49. http://dx.doi.org/10.1016/j.memsci.2005.12.062, URL https://linkinghub.elsevier.com/retrieve/pii/S0376738806000068.

[59] Pazani F, Salehi Maleh M, Shariatifar M, Jalaly M, Sadrzadeh M, Rezakazemi M. Engineered graphene-based mixed matrix membranes to boost CO2 separation performance: Latest developments and future prospects. Renew Sustain Energy Rev 2022;160:112294. http://dx.doi.org/10.1016/j.rser.2022.112294, URL https://linkinghub.elsevier.com/retrieve/pii/S136403212200212X.

[60] Deng M, Zhang Q, Huang Y, Zhang X. Integration and optimization for a PEMFC and PSA oxygen production combined system. Energy Convers Manage 2021;236:114062. http://dx.doi.org/10.1016/j.enconman.2021.114062, URL https://linkinghub.elsevier.com/retrieve/pii/S0196890421002387.

[61] Hasse D, Ma J, Kulkarni S, Terrien P, Tranier J-P, Sanders E, Chaubey T, Brumback J. CO2 capture by cold membrane operation. Energy Procedia 2014;63:186–93. http://dx.doi.org/10.1016/j.egypro.2014.11.019, URL https://linkinghub.elsevier.com/retrieve/pii/S1876610214018347.

[62] Kakoulaki G, Kougias I, Taylor N, Dolci F, Moya J, Jäger-Waldau A. Green hydrogen in Europe – A regional assessment: Substituting existing production with electrolysis powered by renewables. Energy Convers Manage 2021;228:113649. http://dx.doi.org/10.1016/j.enconman.2020.113649, URL https://linkinghub.elsevier.com/retrieve/pii/S0196890420311766.

[63] Sorgulu F, Dincer I. Thermodynamic analyses of a solar-based combined cycle integrated with electrolyzer for hydrogen production. Int J Hydrog Energy 2018;43(2):1047–59. http://dx.doi.org/10.1016/j.ijhydene.2017.09.126, URL https://linkinghub.elsevier.com/retrieve/pii/S0360319917337977.

[64] Wei X, Sharma S, Waeber A, Wen D, Sampathkumar SN, Margni M, Maréchal F, Van Herle J. Comparative life cycle analysis of electrolyzer technologies for hydrogen production: Manufacturing and operations. Joule 2024;S2542435124004252. http://dx.doi.org/10.1016/j.joule.2024.09.007, URL https://linkinghub.elsevier.com/retrieve/pii/S2542435124004252.

[65] Liu H, Clausen LR, Wang L, Chen M. Pathway toward cost-effective green hydrogen production by solid oxide electrolyzer. Energy Environ Sci 2023;16(5):2090–111. http://dx.doi.org/10.1039/D3EE00232B, URL http://xlink.rsc.org/?DOI=D3EE00232B.

[66] Zhan Z, Kobsiriphat W, Wilson JR, Pillai M, Kim I, Barnett SA. Syngas production by coelectrolysis of CO $_2$ /H $_2$ O: The basis for a renewable energy cycle. Energy Fuels 2009;23(6):3089–96. http://dx.doi.org/10.1021/ef900111f, URL https://pubs.acs.org/doi/10.1021/ef900111f.

[67] Hai T, Ashraf Ali M, Alizadeh A, Zhou J, Dhahad HA, Kumar Singh P, Fahad Almojil S, Ibrahim Almohana A, Fahmi Alali A, Shamseldin M. Recurrent neural networks optimization of biomass-based solid oxide fuel cells combined

with the hydrogen fuel electrolyzer and reverse osmosis water desalination. Fuel 2023;346:128268. http://dx.doi.org/10.1016/j.fuel.2023.128268, URL https://linkinghub.elsevier.com/retrieve/pii/S0016236123008815.
[68] Razmi AR, Hanifi AR, Shahbakhti M. Design, thermodynamic, and economic analyses of a green hydrogen storage concept based on solid oxide electrolyzer/fuel cells and heliostat solar field. Renew Energy 2023;215:118996. http://dx.doi.org/10.1016/j.renene.2023.118996, URL https://linkinghub.elsevier.com/retrieve/pii/S0960148123009023.
[69] Wang L, Pérez-Fortes M, Madi H, Diethelm S, Herle JV, Maréchal F. Optimal design of solid-oxide electrolyzer based power-to-methane systems: A comprehensive comparison between steam electrolysis and co-electrolysis. Appl Energy 2018;211:1060–79. http://dx.doi.org/10.1016/j.apenergy.2017.11.050, URL https://linkinghub.elsevier.com/retrieve/pii/S0306261917316367.
[70] Wang L, Düll J, Maréchal F, Van herle J. Trade-off designs and comparative exergy evaluation of solid-oxide electrolyzer based power-to-methane plants. Int J Hydrog Energy 2019;44(19):9529–43. http://dx.doi.org/10.1016/j.ijhydene.2018.11.151, URL https://linkinghub.elsevier.com/retrieve/pii/S0360319918337832.
[71] Wang L, Zhang Y, Li C, Pérez-Fortes M, Lin T-E, Maréchal F, Van Herle J, Yang Y. Triple-mode grid-balancing plants via biomass gasification and reversible solid-oxide cell stack: Concept and thermodynamic performance. Appl Energy 2020;280:115987. http://dx.doi.org/10.1016/j.apenergy.2020.115987, URL https://linkinghub.elsevier.com/retrieve/pii/S0306261920314343.
[72] Clean H. Smart ways for in-situ totally integrated and continuous multisource generation of hydrogen. URL https://switch-fch.eu.
[73] Ma C, Yu H, Monticone G, Ma S, Van Herle J, Wang L. Techno-economic evaluation of biogas-fed SOFC systems with novel biogas purification and carbon capture technologies. Renew Energy 2024;235:121302. http://dx.doi.org/10.1016/j.renene.2024.121302, URL https://linkinghub.elsevier.com/retrieve/pii/S0960148124013703.
[74] SolydEra; URL https://solydera.com/en/business-areas-solutions/.
[75] Sharma S, Rangaiah GP, Maréchal F. Multi-objective optimization programs and their application to amine absorption process design for natural gas sweetening. In: Advances in process systems engineering. second ed.. Vol. 5, World Scientific; 2017, p. 533–60. http://dx.doi.org/10.1142/9789813148239_0016, URL http://www.worldscientific.com/doi/abs/10.1142/9789813148239_0016.
[76] Hasan MMF, Baliban RC, Elia JA, Floudas CA. Modeling, simulation, and optimization of postcombustion CO_2 capture for variable feed concentration and flow rate. 1. Chemical absorption and membrane processes. Ind Eng Chem Res 2012;51(48):15642–64. http://dx.doi.org/10.1021/ie301571d, URL https://pubs.acs.org/doi/10.1021/ie301571d.
[77] Sharma S, Castro-Amoedo R, Hemrle J, Marechal F. Assessment of carbon capture technologies for waste-to-energy system. Comput Aided Chem Eng 2022;51:871–6. http://dx.doi.org/10.1016/B978-0-323-95879-0.50146-6, URL https://www.sciencedirect.com/science/article/pii/B9780323958790501466.
[78] Wei X, Sharma S, Marechal F, Van Herle J. SOFC-VPSA System for Power Generation with CO_2 separation. ECS Trans 2023;111(6):1561–73. http://dx.doi.org/10.1149/11106.1561ecst, URL https://iopscience.iop.org/article/10.1149/11106.1561ecst.
[79] Wei X, Sharma S, Marechal F, Van Herle J. Design and optimization of a shared heat exchanger network for an integrated rSOC system. In: Computer aided chemical engineering. Vol. 52, Elsevier; 2023, p. 1065–70. http://dx.doi.org/10.1016/B978-0-443-15274-0.50170-0, URL https://linkinghub.elsevier.com/retrieve/pii/B9780443152740501700.
[80] Wei X, Sharma S, Waeber A, Van herle J, Marechal F. Integrated solid oxide systems: Advancing efficiency in power generation through fuel cell-electrolyzer coupling with diverse fuels. Comput Aided Chem Eng 2024;53:979–84. http://dx.doi.org/10.1016/B978-0-443-28824-1.50164-2, URL https://www.sciencedirect.com/science/article/pii/B9780443288241501642.
[81] Sharma S, Celebi AD, Maréchal F. Robust multi-objective optimization of gasifier and solid oxide fuel cell plant for electricity production using wood. Energy 2017;137:811–22. http://dx.doi.org/10.1016/j.energy.2017.04.146, URL https://linkinghub.elsevier.com/retrieve/pii/S0360544217307211.
[82] Ma S, Loreti G, Wang L, Maréchal F, Van Herle J, Dong C. Comparison and optimization of different fuel processing options for biogas-fed solid-oxide fuel cell plants. Int J Hydrog Energy 2022;47(1):551–64. http://dx.doi.org/10.1016/j.ijhydene.2021.10.025, URL https://linkinghub.elsevier.com/retrieve/pii/S0360319921039409.
[83] Sharma S, Maréchal F. Robust Multi-Objective Optimization of Solid Oxide Fuel Cell–Gas Turbine Hybrid Cycle and Uncertainty Analysis. J Electrochem Energy Convers Storage 2018;15(4):041007. http://dx.doi.org/10.1115/1.4039944, URL https://asmedigitalcollection.asme.org/electrochemical/article/doi/10.1115/1.4039944/366473/Robust-MultiObjective-Optimization-of-Solid-Oxide.
[84] European Commission Directorate General for Energy, EnergyVille, Vito, Catholic University Leuven, Ghent University, IPESE EPFL, Vrije Universiteit Brussel, DECHEMA. AIDRES, “Advancing industrial decarbonization by assessing the future use of renewable energies in industrial processes”: assessment and geo mapping of renewable energy demand for technological paths towards carbon neutrality of EU energy intensive industries : methodology and results in support to the EU industrial plants database. LU: Publications Office; 2023, URL https://data.europa.eu/doi/10.2833/696697.
[85] Energy Dashboard Switzerland. URL https://www.energiedashboard.admin.ch/preise/gas.
[86] Turton R. Analysis, synthesis, and design of chemical processes. Prentice-hall international series in engineering, Prentice Hall; 2012, URL https://books.google.ch/books?id=f6sbYJuFSycC.
[87] Celebi AD, Sharma S, Ensinas AV, Maréchal F. Next generation cogeneration system for industry – Combined heat and fuel plant using biomass resources. Chem Eng Sci 2019;204:59–75. http://dx.doi.org/10.1016/j.ces.2019.04.018, URL https://linkinghub.elsevier.com/retrieve/pii/S0009250919303847.
[88] Biomass Low cost Advanced Zero Emission small-to-medium scale integrated gasifier fuel cell combined heat and power plant. URL https://www.blazeproject.eu.
[89] Lu S. Economies of scale in PEMEC and SOEC manufacturing based on a bottom-up model. 2022, URL https://infoscience.epfl.ch/handle/20.500.14299/190862.
[90] Liu H, Yu M, Tong X, Wang Q, Chen M. High temperature solid oxide electrolysis for green hydrogen production. Chem Rev 2024;124(18):10509–76. http://dx.doi.org/10.1021/acs.chemrev.3c00795, URL https://pubs.acs.org/doi/10.1021/acs.chemrev.3c00795.
[91] Nwaoha C, Beaulieu M, Tontiwachwuthikul P, Gibson MD. Techno-economic analysis of CO2 capture from a 1.2 million MTPA cement plant using AMP-PZ-MEA blend. Int J Greenh Gas Control 2018;78:400–12. http://dx.doi.org/10.1016/j.ijggc.2018.07.015, URL https://linkinghub.elsevier.com/retrieve/pii/S1750583618303566.
[92] Micari M, Agrawal KV. Oxygen enrichment of air: Performance guidelines for membranes based on techno-economic assessment. J Membr Sci 2022;641:119883. http://dx.doi.org/10.1016/j.memsci.2021.119883, URL https://linkinghub.elsevier.com/retrieve/pii/S0376738821008267.
[93] Luyben WL. Capital cost of compressors for conceptual design. Chem Eng Process - Process Intensif 2018;126:206–9. http://dx.doi.org/10.1016/j.cep.2018.01.020, URL https://linkinghub.elsevier.com/retrieve/pii/S0255270117313168.
[94] Šulc R, Ditl P. A technical and economic evaluation of two different oxygen sources for a small oxy-combustion unit. J Clean Prod 2021;309:127427. http://dx.doi.org/10.1016/j.jclepro.2021.127427, URL https://linkinghub.elsevier.com/retrieve/pii/S0959652621016462.
[95] Shin H, Hansen KU, Jiao F. Techno-economic assessment of low-temperature carbon dioxide electrolysis. Nat Sustain 2021;4(10):911–9. http://dx.doi.org/10.1038/s41893-021-00739-x, URL https://www.nature.com/articles/s41893-021-00739-x.
[96] Songolzadeh M, Soleimani M, Takht Ravanchi M, Songolzadeh R. Carbon dioxide separation from flue gases: A technological review emphasizing reduction in greenhouse gas emissions. Sci World J 2014;2014:1–34. http://dx.doi.org/10.1155/2014/828131, URL http://www.hindawi.com/journals/tswj/2014/828131/.
[97] Park HB, Kamcev J, Robeson LM, Elimelech M, Freeman BD. Maximizing the right stuff: The trade-off between membrane permeability and selectivity. Science 2017;356(6343):eaab0530. http://dx.doi.org/10.1126/science.aab0530, URL https://www.science.org/doi/10.1126/science.aab0530.
[98] Jackson S, Brodal E. A comparison of the energy consumption for CO_2 compression process alternatives. IOP Conf Ser: Earth Environ Sci 2018;167:012031. http://dx.doi.org/10.1088/1755-1315/167/1/012031, URL https://iopscience.iop.org/article/10.1088/1755-1315/167/1/012031.
[99] Maréchal F, Kalitventzeff B. Energy integration of industrial sites: tools, methodology and application. Appl Therm Eng 1998;18(11):921–33. http://dx.doi.org/10.1016/S1359-4311(98)00018-0, URL https://linkinghub.elsevier.com/retrieve/pii/S1359431198000180.
[100] Wallerand AS, Kermani M, Kantor I, Maréchal F. Optimal heat pump integration in industrial processes. Appl Energy 2018;219:68–92. http://dx.doi.org/10.1016/j.apenergy.2018.02.114, URL https://linkinghub.elsevier.com/retrieve/pii/S0306261918302393.
[101] Kermani M, Wallerand AS, Kantor ID, Maréchal F. Generic superstructure synthesis of organic Rankine cycles for waste heat recovery in industrial processes. Appl Energy 2018;212:1203–25. http://dx.doi.org/10.1016/j.apenergy.2017.12.094, URL https://linkinghub.elsevier.com/retrieve/pii/S0306261917318172.
[102] Blvd W, Va A. Manufacturing cost analysis of stationary fuel cell systems. 2012, URL https://www.hydrogen.energy.gov/pdfs/review11/fc018_james_2011_o.pdf.
[103] Shi L, Zhao Y, Matz S, Gottesfeld S, Setzler BP, Yan Y. A shorted membrane electrochemical cell powered by hydrogen to remove CO2 from the air feed of hydroxide exchange membrane fuel cells. Nat Energy 2022;7(3):238–47. http://dx.doi.org/10.1038/s41560-021-00969-5, URL https://www.nature.com/articles/s41560-021-00969-5.
[104] Caliandro P, Tock L, Ensinas AV, Marechal F. Thermo-economic optimization of a Solid Oxide Fuel Cell – Gas turbine system fuelled with gasified lignocellulosic biomass. Energy Convers Manage 2014;85:764–73. http://dx.doi.org/10.1016/j.enconman.2014.02.009, URL https://linkinghub.elsevier.com/retrieve/pii/S0196890414001186.
[105] Lee G, Li YC, Kim J-Y, Peng T, Nam D-H, Sedighian Rasouli A, Li F, Luo M, Ip AH, Joo Y-C, Sargent EH. Electrochemical upgrade of CO2 from amine capture solution. Nat Energy 2020;6(1):46–53. http://dx.doi.org/10.1038/s41560-020-00735-z, URL https://www.nature.com/articles/s41560-020-00735-z.